

Journal Pre-proofs

Research papers

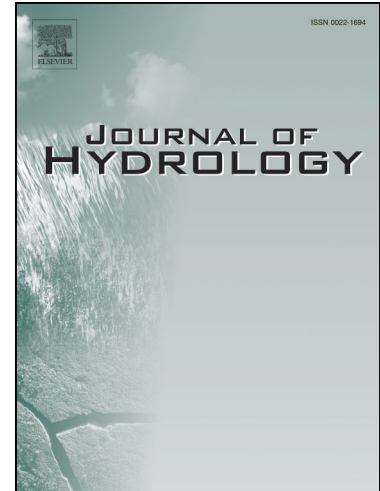
Evaluation of water temperature under changing climate and its effect on river habitat in a regulated Alpine catchment

F. Fuso, L. Stucchi, L. Bonacina, R. Fornaroli, D. Bocchiola

PII: S0022-1694(22)01386-5

DOI: <https://doi.org/10.1016/j.jhydrol.2022.128816>

Reference: HYDROL 128816



To appear in: *Journal of Hydrology*

Received Date: 7 June 2022

Revised Date: 7 November 2022

Accepted Date: 8 November 2022

Please cite this article as: Fuso, F., Stucchi, L., Bonacina, L., Fornaroli, R., Bocchiola, D., Evaluation of water temperature under changing climate and its effect on river habitat in a regulated Alpine catchment, *Journal of Hydrology* (2022), doi: <https://doi.org/10.1016/j.jhydrol.2022.128816>

This is a PDF file of an article that has undergone enhancements after acceptance, such as the addition of a cover page and metadata, and formatting for readability, but it is not yet the definitive version of record. This version will undergo additional copyediting, typesetting and review before it is published in its final form, but we are providing this version to give early visibility of the article. Please note that, during the production process, errors may be discovered which could affect the content, and all legal disclaimers that apply to the journal pertain.

Evaluation of water temperature under changing climate and its effect on river habitat in a regulated Alpine catchment

F. Fuso ^{a, *}, L. Stucchi ^{a, *}, L. Bonacina ^b, R. Fornaroli ^b, and D. Bocchiola ^a

a. Department of Civil and Environmental Engineering, Politecnico di Milano, Milano, Italy.
flavia.fuso@polimi.it; leonardo.stucchi@polimi.it; daniele.bocchiola@polimi.it

b. Department of Earth and Environmental Sciences, University of Milano Bicocca, Milano, Italy.
l.bonacina9@campus.unimib.it; riccardofornaroli@gmail.com

* Correspondence: leonardo.stucchi@polimi.it

Abstract

Habitat quality of alpine river is largely affected by human activity. The exploitation for hydropower, combined with anthropogenic climate change, can alter mountain riverine ecosystems, leading to less suitable hydro-thermal regimes for the fish. Here, we present a new methodology to assess water temperature within a river featuring water exploitation for hydropower purposes, usable to assess future potential deterioration of riverine habit suitability in response to (increasing) water temperature. We then propose an application focusing upon the case study of the Serio River, in Northern Italy, largely exploited by hydropower productions and highly populated by a very sensitive species, brown trout (*Salmo trutta*). The methodology proposed involves a set of tools, i.e. i) the hydrological model *Poli-Hydro*, to evaluate natural hydrological regime, ii) a hydropower plants scheme to assess river water withdrawal, iii) fish density-environment curves to evaluate the hydraulic suitability in terms of trout potential density for adult, young, and fry as a function of hydraulic features, i.e. depth and velocity, and iv) a new, physically based model, *Poli-Wat.Temp*, to assess changes in river water temperature, and possible outbreaks of temperature dependant lethal conditions, such as proliferative kidney disease, and others. To provide an assessment of river suitability, possibly complementing (improving?) models based upon solely hydraulic indexes, we propose a new synthetic River Stress index, combining i)

26 potential fish density as driven by hydraulic variables, and ii) thermal suitability. Given that utmost
27 unsuitable conditions (thermally, and likely hydrologically) are expected under future climate conditions
28 pending global warming, we then projected water temperature, and stream flows until the end of the
29 century, in response to socio-economic scenarios of AR6 of the IPCC, to explore the potential for future
30 decrease of river quality. Water temperature would be largely susceptible to climate change with increase
31 up to +6.5 C° in the worst scenarios, while no clear trend is observed for fish density. Overall, potential
32 density would decrease in winter for adults, and in summer for juvenile and fry in downstream sections.
33 Therefore, by coupling hydraulic, and thermal suitability, one finds that i) Alpine rivers would likely face
34 longer critical periods, with respect to those predicted based upon a solely hydraulic habitat based
35 assessment, and ii) continuous temperature increase as projected until the end of the century would result
36 into worse conditions in summer months, seriously endangering fish guilds.

37

38 **Keywords**

39 Water temperature modelling; Physical habitat modelling; River stress indicator; Climate change

40

41 **1. Introduction**

42 Global warming effects upon water ecosystems have now been evident for years. The impact of climate
43 change on freshwater availability was assessed both at regional (Arnell, 1999; Lehner et al., 2006), and
44 global scale (Doll and Zhang, 2010; Sperna et al., 2012; Vorosmarty et al., 2000). Among others, several
45 studies were carried out that highlighted significant warming in the European Alps, decreasing of snow
46 and ice cover, and stream flows modification thereby (Bocchiola and Diolaiuti, 2010; Bocchiola, 2014;
47 Fuso et al., 2020). Few studies focused upon changes of water temperature, which is crucial for the
48 distribution of biotic organisms in the rivers, featuring direct and indirect effects. Beside the direct

49 influence upon dissolved oxygen (Webb et al., 2008; Van Vliet et al., 2013), increase in water
50 temperature may provide emergence of diseases, such as proliferative kidney disease PKD in freshwater
51 fish (Carraro et al., 2017). PKD is a major threat to wild and farmed salmonid populations because of its
52 lethal effect at high water temperatures. The disease was recognized as a frequent cause of decline in fish
53 populations over the last decades, even driving local extinctions of endemic and/or commercially
54 important fish species (Borsuk et al., 2006).

55 When studying thermal regime of rivers, attention was cast hitherto upon the link between water, and air
56 temperature. The latter can indeed be seen as a driver of the former, because it affects heat flows to/from
57 water (Edinger et al., 1968; Zhu et al., 2018). Thus, projected air temperature increase under global
58 warming will likely affect mountain streams temperature, and living conditions of river species (Isaak et
59 al., 2010; Santiago et al., 2016; Borgwardt et al., 2020). Stochastic models exist that link water and air
60 temperature, and are easy to implement, thanks to the large diffusion of air temperature data (Caissie et
61 al., 2001, Caissie et al., 1998). Further meteorological data are needed to apply more sophisticated
62 deterministic models based upon energy balance (Caissie et al., 2005, Bustillo et al., 2015). However,
63 the latter are more appropriate to analyse anthropogenic activities directly impacting rivers, e.g.,
64 diversion channels, industrial flows, and presence of reservoirs (Benyahya et al., 2007). Dams and minor
65 barriers disrupt the hydrological and fluvial ecosystem connectivity, affecting the river environment, and
66 thermal regime (Kedra and Wiejackza, 2017). Particularly, diverted water is less susceptible to heating,
67 given that often times diversion channels are buried in the ground. Then, return of such colder water in
68 the main river (typically at some length downstream, and at a lower altitude) would cause a sudden drop
69 in water temperature. On the other hand, water flow left in the river has less thermal inertia due to
70 decreased discharge, leading to higher temperature in summer, and lower in winter (Meier et al., 2003).
71 Thermal models depending upon air temperature only may not be always suitable, i.e. the effect of flow

72 magnitude cannot be neglected (Toffolon and Piccolroaz, 2015), and more sophisticated heat exchange
73 models are required, that make spatial dependence and effects of increasing flow downstream more
74 explicit.

75 The EU Biodiversity strategy for 2030 (EC, 2020) states the need to re-establish freshwater ecosystems,
76 and the natural functions of rivers. In this context, the assessment of river habitat quality is a key factor
77 (Lamouroux et al., 1998, Canobbio et al., 2013), and one expects that fish distribution/abundance will
78 reflect riverine conditions on a larger spatial scale (Lamouroux and Cattaneo, 2006, Van Compernelle et
79 al., 2019). Physical habitat models have been widely used to describe the connection between instream
80 flow and habitat availability for different target species (Fornaroli, 2016). However, in addition to
81 hydrological flows, water temperature is determinant for river species occurrence (Nukazawa et al., 2011,
82 Jonsson B. et Jonsson N., 2009). Thus, to simulate habitat suitability, it seems relevant to consider
83 multiple habitat characteristics, and integrated frameworks that couple water temperature and hydraulic
84 parameters may be considered (Morid et al., 2020).

85 The main goals of our study are 1) to propose a new physically based thermal model, called *Poli-*
86 *Wat.Temp* to assess water temperature of a river characterized by complex geometry of withdrawal, and
87 return to/from hydropower plants, and 2) to evaluate the combined effect of hydraulic, and thermal stress
88 upon mountain river habitat, by elaborating a new index, which we call *River stress*.

89 We develop here the method and then we propose an application to a stretch of an Alpine river, the Serio
90 catchment in northern Italy. We chose this catchment for two reasons, i.e. i) it nests several hydropower
91 plants, displaying a complex geometry of diversion/return channels, affecting both hydrological and
92 thermal regimes, and ii) it is populated by *Salmo trutta*, the presence of which is nowadays made possible
93 by high dissolved oxygen and somewhat acceptable water temperature (Armour, 1994). The thermal
94 model was calibrated using field data of air and water temperature, taken during surveys in several cross

95 sections along the Serio River. River discharge at several chosen locations along the stream was assessed
96 using the semi-distributed, physically based hydrological model *Poli-Hydro* (Soncini et al., 2017) at the
97 basin scale. For habitat quality assessment, we then used the so modelled discharges as an input to
98 density-environmental functions for *Salmo trutta* at different stages (young, adult, and fries), calibrated
99 recently for the Serio River (Fornaroli et al., 2016), to then evaluate the limiting effects of hydro-
100 morphological variables, such as water depth, current velocity, substrate size and composition, upon
101 habitat conditions. We then propose a new index of river stress, by combining habitat suitability and
102 water temperature, so obtaining more credible habitat assessment under given climate conditions.
103 We projected water temperatures, and stream flows to the end of the XXI century, in response to climate
104 change as projected under the socio-economic scenarios (SSP) of the most recent assessment report
105 (AR6) of the Intergovernmental panel on climate change (IPCC), to highlight areas of increased stress,
106 usable for future planning of adaptation strategies. The paper is organized as follows. The case study and
107 available data are reported in section 2, where also the methods are discussed. The results of model
108 calibration, and subsequent of application are discussed in Section 3. Discussion, and conclusions are in
109 sections 4, and 5, respectively.

110

111 **2. Materials and methods**

112 2.1. Case study

113 Serio River is 124 km long, nested in Lombardy region (northern Italy), flowing in the provinces of
114 Bergamo (BG) and Cremona (CR), to the outflow of the Adda River (Figure 1). It has a watershed of
115 1256 km², and the source is located at 2500 m asl nearby Torena mount, in the Orobic Prealps. Serio is
116 a mountain river, with mono-cursal bed, step-pools geometry, and coarse substrate. At ca. 600 m asl in
117 Parre (BG), the river becomes more and more braiding, and gravel/sand bottomed. At ca. 100 m asl, it

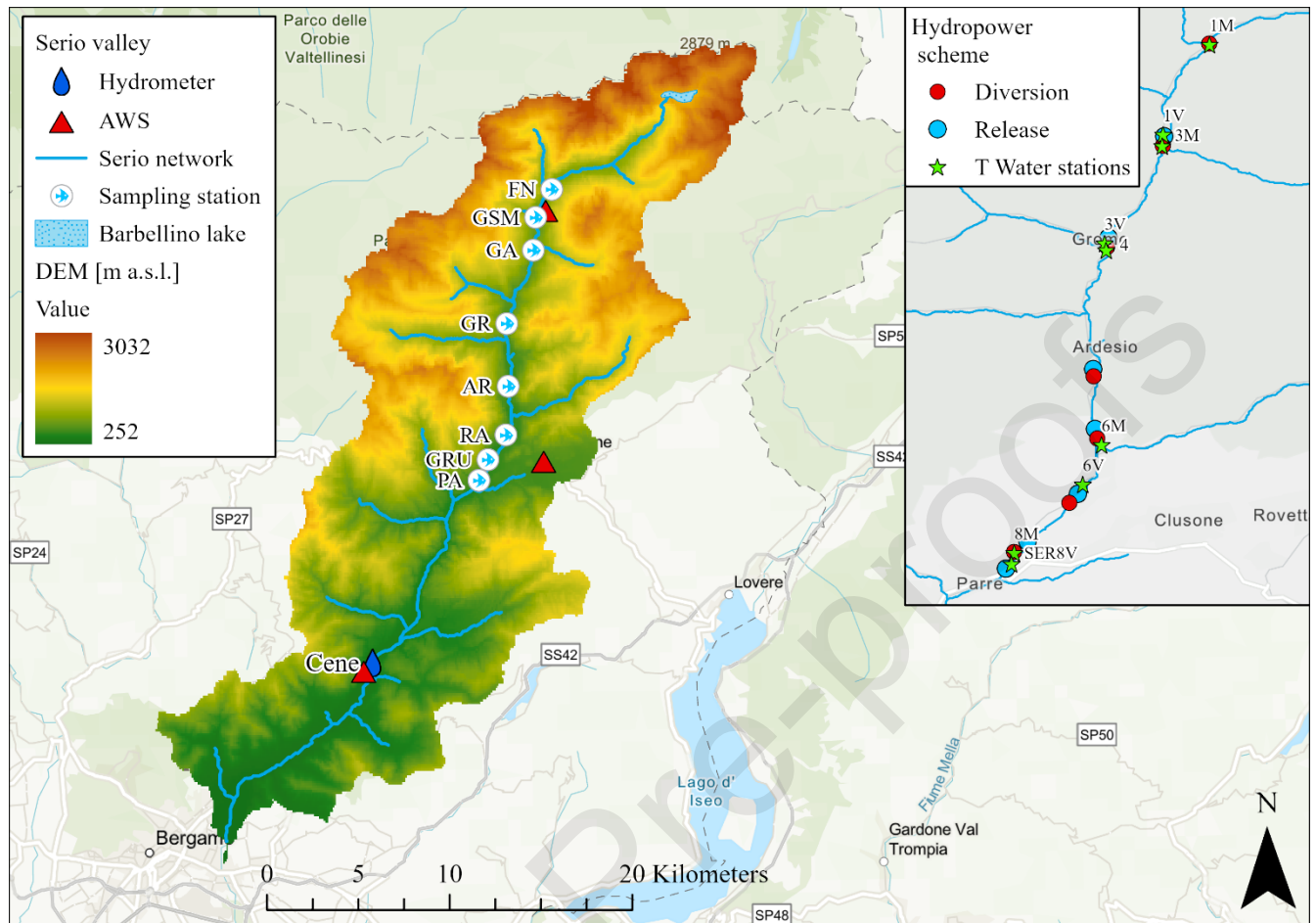
118 starts meandering with very gentle slope, and fine substrate. Here we consider the river stretch upstream
119 of Parre, most relevant for water quality assessment, and for measurable presence of the target fish
120 species.

121 The watershed is located within a temperate region, with a total precipitation of ca. 1300 mm per year,
122 and mean temperature of +23.8 °C in July, and -1.5°C in January. The river receives large precipitation
123 in autumn, and large snow melt in spring. No ice melt contribution is present here, due to the absence of
124 permanent glaciers in the area. The hydrological regime displays low discharges in January and February,
125 mild flow in spring, and main floods in fall.

126 The Serio River is largely exploited for hydropower production. Seven run of river power plants are
127 located along the river that we know of, in Valbondione to Parre stretch (Figure 1). The water collecting
128 and returning points form 7 stretches, where the hydrological and thermal regime is altered with respect
129 to natural conditions.

130 The considered reach is classified as a “high regard” area for fishing by the province of Bergamo (2009),
131 where the most valued fish species is Brown Trout (*Salmo trutta*), protected from overfishing by a
132 limitation in time and amount (Lombardy region, 2003). Changes in precipitation and temperature may
133 negatively affect the hydrological regime of the area (Armour, 1994, Viganò et al., 2016, Gropelli et
134 al., 2011), leading to critical hydro-thermal conditions for the fish. It is therefore essential to study the
135 impact of such present, and potential future changes upon river quality, to plan adaptation strategies for
136 safeguarding of the species and their ecosystem.

137 Here, we assessed the effect of climate change upon river habitat within 8 stations of the Upper Serio
138 (Figure 1), where hydro-morphological and topographic surveys, together with electro fishing samplings
139 were carried out, as described e.g. in Viganò et. al (2016).



140

141

142

143

144

145

2.2. Data available

146

147

148

149

150

Figure 1. Catchment area of Serio River. We report the position of automatic weather stations (AWSs), hydrometric stations, sampling station for fish habitat assessment, and water temperature sampling stations, and as well a scheme of the hydropower diversion-restitution system. Geographic Reference System WGS 84.

Daily series of precipitation, and air temperature from 3 automatic weather station (AWS) of ARPA Lombardy Authority were used here as inputs to the hydrological model *Poli-Hydro* (e.g. 9). The model was implemented with a spatial resolution of $100 \times 100 \text{ m}^2$, for a 10 year control run period (CR), 2012-2021. Other inputs were the GIS map, i.e. digital elevation model (DEM) of the catchment (Earth data Available online: <https://earthdata.nasa.gov/>), and the land use maps from CORINE land cover (CLC

151 2018 — Copernicus Land Monitoring Service Available online: <https://land.copernicus.eu/pan->
 152 [european/corine-land-cover/clc2018](https://land.copernicus.eu/pan-european/corine-land-cover/clc2018)). Daily discharges at Ponte Cene hydro station during the CR period
 153 were used for model calibration under natural regime conditions, while data of Minimum Instream Flow
 154 (MIF) and maximum operable discharge (Q_{HY}) for each hydropower station were used to switch from
 155 natural, to regulated hydrological regime (Table 1).

156 To setup the thermal model, water temperature data were gathered within the sites reported in Figure 1
 157 (see Table 2), for three years (June 2018-October 2021), using *iButton* devices (range -5 to +26 °C,
 158 resolution: $\pm 0.0625^\circ\text{C}$, measurement interval 10 min). Water temperature data were downloaded, and a
 159 linear interpolation between consecutive measurements was performed to obtain a continuous trend of
 160 water temperature (one value per minute), and eventually daily mean, maximum and minimum
 161 temperature. Finally, density-environmental relationships for *Salmo trutta* at different stages (fry,
 162 juvenile, adult) as derived after sampling in eight stations along the river (Fornaroli et al., 2016) were
 163 used for river habitat assessment (Table 1).

Station	ID	Longitude	Latitude	Altitude m a.s.l.	MIF [m^3s^{-1}]	Q_{HY} [m^3s^{-1}]
Fiumenero	FN	9.96°	46.02°	788	0.4	4.5
Gromo San Marino	GSM	9.95°	46.01°	750	0.4	4.5
Gandellino	GA	9.94°	45.99°	687	0.6	4.5
Gromo	GR	9.93°	45.95°	604	0.9	9.7
Ardesio	AR	9.93°	45.92°	542	1	8
Rasini	RA	9.92°	45.90°	537	1.1	12
Grumella	GRU	9.91°	45.89°	495	1.3	11
Parre	PA	9.90°	45.88°	487	1.5	10.3

164

165 *Table 1. Fish sampling stations with acronym and location. For each station are reported the values of Minimum Instream*

166 *Flow (MIF) and maximum operable discharge (Q_{HY}) of hydropower plant affecting the station.*

ID	Longitude	Latitude	Altitude
			m a.s.l.
1M	9.959°	46.021°	789
1V	9.946°	45.996°	691
3M	9.946°	45.993°	692
3V	9.930°	45.966°	635
4	9.930°	45.964°	626
6M	9.929°	45.910°	516
6V	9.924°	45.899°	503
8M	9.905°	45.880°	491
8V	9.904°	45.877°	486

Table 2 Water temperature stations (from upstream to downstream). Coordinates in WGS84.

167

168

169

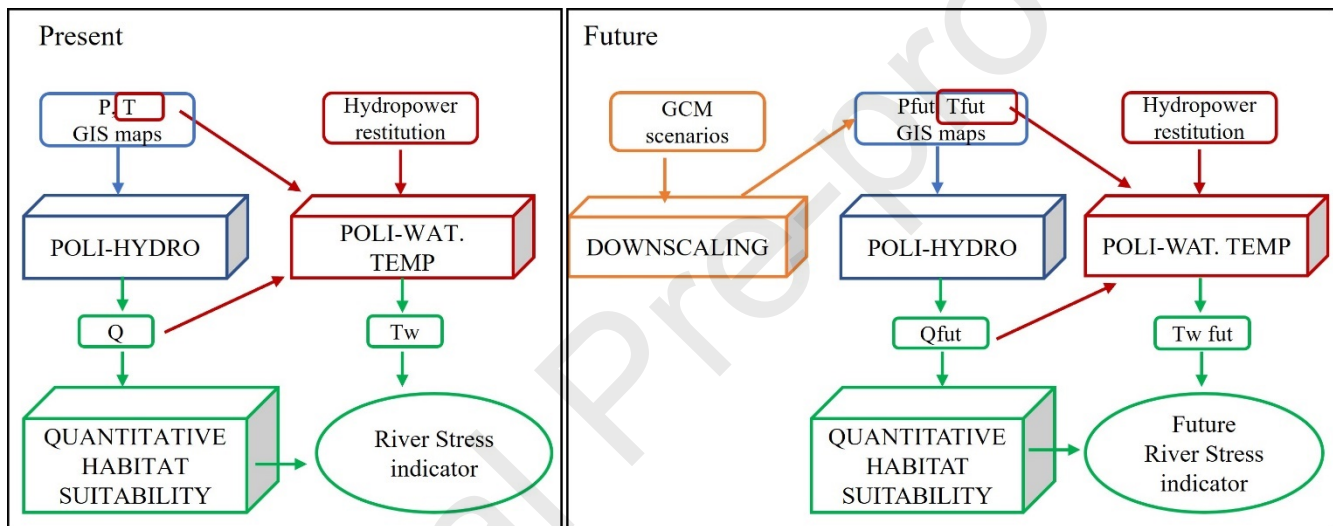
170 2.3. River suitability assessment

171 To assess the river suitability of Serio River several methods/models were applied here in cascade. For
 172 clarity, we report in Figure 2 a flowchart displaying the data and methods adopted here.

173 Using precipitation and air temperature data (P, T), and watershed GIS maps we setup the hydrological
 174 model *Poli-Hydro*, to derive daily discharges Q. We used then the modelled discharges as input to a
 175 habitat suitability model that defines fish potential density, used to evaluate habitat suitability in the
 176 sample locations. With the thermal model, based upon known the geometry of the hydropower system,
 177 and of the return (tail-race) system, we then used T, and the modelled discharge Q, to assess pointwise
 178 daily water temperature T_w . Then, we defined habitat suitability classes and water temperature thresholds

179 for PKD. Next, we provided an indicator of stress of the river RS , by matching hydraulic habitat
 180 suitability, with suitability based upon water temperature, which we call TS . For future projections, we
 181 downscaled values from GCM scenarios to get future precipitation, and temperature, P_{fut} and T_{fut} . These
 182 were fed to *Poli-Hydro* to assess future discharges Q_{fut} . Still using the thermal model, we then exploited
 183 T_{fut} , Q_{fut} , to evaluate future scenarios of water temperature $T_{w,fut}$, and suitability thereby. Here, we
 184 assumed for simplicity that the present hydropower scheme would remain unchanged in the future.
 185 Finally, with the same approach above, we provided projections of the future river stress RS_{fut} .

186



187

Figure 2. Flowchart of the methodology adopted for present and future river stress assessment.

188

189 2.4. Hydrological modelling

190 The *Poli-Hydro* hydrological model was already used, validated, and described in several studies hitherto
 191 (Soncini et al., 2017), where the reader is referred thereby for a detailed description. *Poli-*
 192 *Hydro* computes daily soil water balance for each cell within the catchment area (here defined with ARC-
 193 GIS software). The control variable is soil water content, inputs are given by liquid precipitation, air
 194 temperature, and snow/ice melt, and outputs are water fluxes in the river. Snow accumulation on the

195 ground, in the form of Snow Water Equivalent (SWE) is assessed from precipitation, i.e. snowfall when
 196 temperature in one cell is below 0°. SWE melt is then evaluated with a mixed degree day formula (e.g.
 197 Pellicciotti et al., 2005). Temperature is distributed spatially using monthly vertical gradients as from
 198 observations. By doing so, the model can reconstruct for each cell rainfall, snow pack on the ground,
 199 snow/ice melt (however as reported, no ice surface is present in the catchment here), surface
 200 and subsurface flows. The latter are then routed (using a IUH function, i.e. Nash model) to the final outlet
 201 of each sub-basin, to obtain daily stream flow hydrographs. The model was calibrated here for natural
 202 discharge estimation, and then validated using goodness of fit statistics, i.e. *Bias*, and monthly
 203 *NSE* (Nash-Sutcliffe Efficiency) calculated against the observed discharges at Ponte Cene hydrometer,
 204 relatively undisturbed by flow regulation, and simulated discharges. To include water withdrawal from
 205 hydropower stations, for each location, we assumed that 90% of the discharge above minimum instream
 206 flow (i.e. ecological flow) MIF is diverted, until maximum operable flow (Equation 1).

$$\begin{aligned}
 Q &= Q_{nat} && \text{if } Q_{nat} < Q_{MIF} \\
 Q &= (Q_{nat} - Q_{MIF}) \cdot 10\% + Q_{MIF} && \text{if } Q_{MIF} < Q_{nat} < Q_{HY} \\
 Q &= Q_{nat} - Q_{HY} && \text{if } Q_{nat} > Q_{HY}
 \end{aligned} \tag{1}$$

207
 208 Here Q is actual river discharge to be assessed, and Q_{nat} is natural discharge as evaluated by *Poli-Hydro*.
 209 Q_{MIF} is Minimum Instream Flow value, specific for each power plant, and Q_{HY} is maximum discharge
 210 conveyed to the power plants. As per regulation of Lombardy region, Q_{MIF} is provided for every plant
 211 (Table 1), and we used the proposed values accordingly, in the assumption that hydropower managers
 212 properly release Q_{MIF} downstream of intakes.

213

214 2.5. Hydraulic habitat assessment

215 To assess hydraulic based suitability, we used a habitat suitability model that defines potential density
216 based upon a limiting factor approach, as recently proposed by Fornaroli et al. (2016). These functions
217 use water velocity/depth, substrate characteristics, availability of refuges, and mesohabitat type. The
218 latter is divided in four categories, namely i) Shallow pool, ii) Deep pool, iii) Riffle, iv) Run, as retrieved
219 within the 8 sampling sites (Figure 1, Table 1). Using the functions as developed in our study area
220 (Fornaroli et al., 2016) we assessed the potential density (PD) (ind/m^2) with respect to discharge for the
221 young and adult trout, and for fries, obtaining a potential number of individuals per square meters in each
222 site, for each discharge level. So, we calculated *PD* for the CR period in each sampling site, and for each
223 life stage of *Salmo trutta*. We then defined two classes of quality, i.e. poor and good, corresponding to
224 the intervals for PD 40-60%, 60-100%, of the maximum value of daily potential density PD_{max} ,
225 respectively. We chose 40% as a lower bound, because it was the lowest value resulting from our
226 simulations. Thus, we added up the total number of days in each class, for the 4 seasons (winter, spring,
227 summer, and fall) and we averaged over three different decades, i.e. CR (2012-2021) as a reference in
228 the present conditions, a period one P1, half century (2046-2055), and a period two P2, end of century
229 (2091-2100), to evaluate future river suitability.

230

231 2.6. Water temperature modelling

232 Here we developed a model for water temperature assessment, which we called *Poli-Wat.Temp*. This is
233 a coupled model, interacting with *Poli-Hydro*, to take as an input estimated stream flows, and air
234 temperature data. The *Poli-Wat.Temp* model uses a one-dimensional energy balance equation, suitable
235 for shallow rivers where vertical gradient of temperature can be neglected (Caissie et al., 2005), as
236 follows:

$$\frac{\partial T_w}{\partial t} + v \cdot \frac{\partial T_w}{\partial x} - \frac{1}{A} \cdot \frac{\partial}{\partial x} \left(A \cdot D_L \cdot \frac{\partial T_w}{\partial x} \right) = \frac{B}{\theta \rho A} \cdot H_{tot} \quad (2)$$

237

238 Therein, T_w is water temperature, v is mean water velocity, x is distance along river axis, A is cross
 239 section area, B is river width, D_L is a dispersion coefficient in the flow direction, θ is specific heat of
 240 water, ρ is water density, H_{tot} is total heat flux from the external environment to the river, including solar
 241 radiation, air temperature, evaporative heat fluxes, and net long-wave radiation. Here, we considered air
 242 temperature, and incident solar radiation as external sources of heat, that we modelled as linear functions
 243 of the air-water temperature gradient, and of incident, clear sky solar radiation, respectively

$$H_{tot} = \alpha \cdot (T_{air} - T_w) + \beta \cdot Rad \quad (3)$$

244

245 The dispersion term in Eq. 2 $\partial(A \cdot D_L \cdot \partial T_w / \partial x) / \partial x$ may be generally neglected in alpine rivers,
 246 characterized by medium/high flow velocity, so that heat transfer along the x axis basically occurs by
 247 advection (Deas and Lowney, 2000) $v \cdot \partial T_w / \partial T_w$.

248 We solved Eq. 2 recursively, to evaluate heat fluxes from an upstream station to a downstream one, with
 249 temperature T_{w1} , and T_{w2} respectively, using a finite differences scheme, where ∂x was approximated
 250 with the distance L between the considered stations, and ∂t is 1 day.

251 Using a first-order upwind scheme, and approximating river channel shape with a rectangular one,
 252 roughly valid for naturally shaped rivers, such as Serio River here in several traits, we moved from
 253 Equation 2 to Equation 4, and then isolated $T_{w2,i2}$ to explicitly assess downstream temperature at day 2
 254 (Eq. 5).

$$(T_{w1,i2} - T_{w1,i1})/\Delta t + v/L \cdot (T_{w2,i2} - T_{w1,i2}) = \frac{1}{\theta\rho h} \cdot (\alpha \cdot (T_{air} - T_{w1,i2}) + \beta \cdot Rad_{i2}) \quad (4)$$

$$T_{w2,i2} = T_{w1,i2} + \frac{L}{v\Delta t\theta\rho h}(\alpha \cdot (T_{air} - T_{w1,i2}) + \beta \cdot Rad_{i2}) - \frac{L}{v\Delta t}(T_{w1,i2} - T_{w1,i1}) \quad (5)$$

255 Therein $i1$, $i2$ indicate day 1, and 2, and h is water depth. The water depth, and the velocity v could be
 256 evaluated as (power) functions of discharge. In this space dependant formulation, one needs to fix an
 257 upstream initial condition for temperature. Therefore, we set the initial condition of the temperature at
 258 the largest lake upstream, i.e. Barbellino lake, where changes in temperature are more gradual and season
 259 dependant. The Barbellino reservoir is an artificial lake located at 1870 m a.s.l., 9.3 km upstream of the
 260 first thermal station, where outflow is regulated by a hydropower dam, 69 m tall. Serio River starts at the
 261 toe of the Serio waterfall (with a 315 m jump, i.e. the tallest waterfall of Italy) watered with the reservoir
 262 output. Generally, due to thermocline water temperature at a depth of 20+ m can be taken as constant, at
 263 +4° C (Dodds et Whiles, 2010). However, withdrawal from the bottom outlet has a mixing effect that
 264 has been shown to impact upon *hypolimnion* (lake bottom) temperature (Saber et al., 2019, Nurnberg).
 265 Therefore, here we modelled Barbellino hypolimnion temperature using a sinusoidal function, well
 266 representing lake bottom temperature in other regulated lakes (48). Therein, minimum water temperature
 267 can be fixed at +4 °, and phase, amplitude and mean values are related to seasonal air temperature as

$$T_{wBar} = \gamma\bar{T}_y + \omega(\bar{T}_{sum} - \bar{T}_y) \cdot \sin\left(2\pi\frac{day - lag}{365} - \pi\right) \quad (6)$$

268 Therein, \bar{T}_y and \bar{T}_{sum} are annual, and July mean temperature estimated at Barbellino lake, that we linked
 269 to average, and summer variation of water temperature, respectively. Also, γ, ω, lag are calibration
 270 parameters. For model tuning, we used data of water temperature at the station of Fiumenero.

271 As mentioned above, along the river stem several hydropower plants divert water, modifying stream
 272 flows, and temperature thereby. To account for this, the thermal balance as from Eq. 5 was further
 273 modified to consider stream flow changes between different sections, as due to i) hydrological flow
 274 increase (contributing catchment), ii) water diversion for hydropower, and iii) water return from
 275 hydropower (tail race channels). The water used for hydropower in Serio River is often collected in
 276 channels buried in the ground, i.e. largely insulated from the atmosphere, and restitution at lower altitude
 277 occurs quite rapidly with respect to stream flow dynamics (i.e. with a shorter delay than the time span
 278 required for the river flow to reach the same altitude). Accordingly, we made the hypothesis that
 279 diverted/returned water keeps the same temperature, i.e. the water temperature at the restitution point is
 280 the same as the (stream) temperature at the point of withdrawal. One can thereby assess water temperature
 281 downstream of a flow returning point (i.e. downstream of a tail race channel) as the weighted average of
 282 the upstream (in river) temperature, and the tail race temperature as

$$T_{w3} = \frac{T_{w1} \cdot Q_1 + T_{w2} \cdot Q_2}{Q_1 + Q_2} \quad (7)$$

283
 284 Here, T_{w3} is water the temperature downstream tail race, and T_{w1}, T_{w2} are temperature of instream and
 285 diverted water, and Q_1, Q_2 are discharge values thereby.

286

287 2.7. Critical temperature for thermal suitability

288 In this case of study, where *Salmo Trutta* is abundant, and oxygen rate during our ten-year campaign was
 289 always found at saturation level due to the high water turbulence of many riffles/rapids, we chose as a
 290 target disease PKD, being particularly temperature dependant (Waldner et al., 2019), and a main threat
 291 for Alpine trouts (e.g. Wahli et al., 2007). To define the critical thresholds of water temperature for PKD
 292 we relied upon the most recent literature (Carraro et al., 2017, Santiago et al., 2016, Borgwardt et al.,
 293 2020), and we decided to use the criteria as set out by Borgwardt et al. (2020), considering water
 294 temperature T_w , and a corresponding consecutive duration d_{T_w} .

295 When the daily mean temperature is above $T_w \geq +15^\circ\text{C}$, a situation of i) *possible outbreak* of PKD occurs
 296 if the exceedance lasts for $d_{T_w} \geq 14$ consecutive days (Eq. 8), and a situation of ii) *low mortality* occurs
 297 when $d_{T_w} \geq 29$ consecutive days (Eq. 9). The most worrisome condition, i.e. iii) *high mortality*, takes
 298 place when the daily mean temperature exceeds $T_w \geq +18^\circ\text{C}$ and $d_{T_w} \geq 26$ consecutive days (Eq. 10).

$$\text{Possible Outbreak: } T_w \geq +15^\circ\text{C} \cap d_{T_w} \geq 14 \quad (8)$$

$$\text{Low Mortality: } T_w \geq +15^\circ\text{C} \cap d_{T_w} \geq 29 \quad (9)$$

$$\text{High Mortality: } T_w \geq +18^\circ\text{C} \cap d_{T_w} \geq 29 \quad (10)$$

299

300 2.8. River stress indicator

301 To provide a more comprehensive habitat assessment under present, and future climate, we constrained
 302 habitat suitability upon water temperature, by calculating a River Stress indicator RS, representing the
 303 number of days per year when the river is in stress conditions. RS is defined as the union of i) days of
 304 poorest river quality, e.g. number of days when PD is 40-60% of PD_{\max} , and days when ii) water
 305 temperature is above the lowest threshold for PKD occurrence, e.g. possible outbreak, ideally more
 306 responsive to climate change.

$$RS = 0.4 PD_{max} \leq PD \leq 0.6 PD_{max} \cup (T_w \geq +15^\circ\text{C} \cap d_{T_w} \geq 14) \quad (11)$$

307 We calculated the total number of days when the river would be in a poor quality conditions at each
 308 sampling site, for the 4 seasons, and we averaged this number on the three reference decades, CR (2012-
 309 2021), P1(2046-2055), and P2 (2091-2100).

310

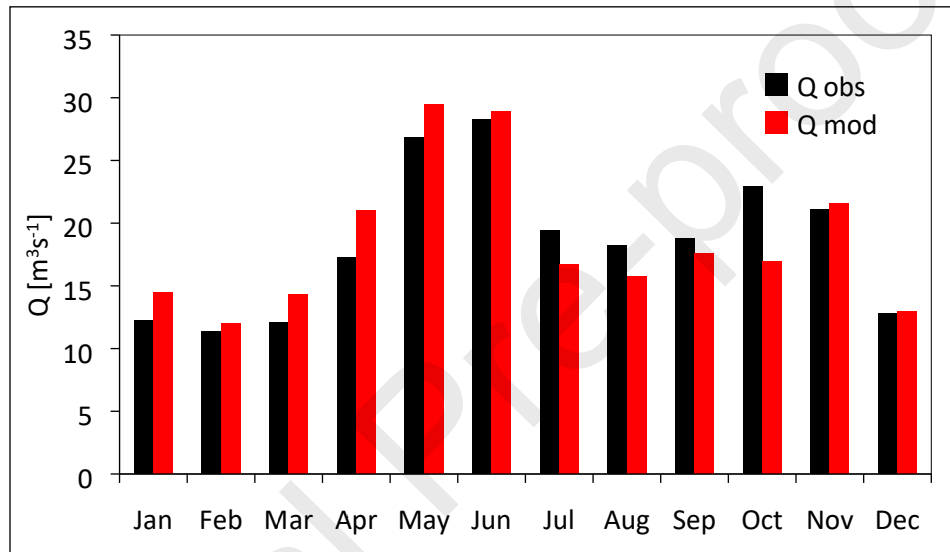
311 2.9. Hydrological projections

312 To evaluate future air temperature to constrain hydrological scenarios we performed a downscaling of
 313 the outputs from six Global Circulation Models (GCMs), from the last Assessment Report 6 (AR6) of
 314 the IPCC, namely European EC-Earth3.0 (EC-Earth), CESM2 (Danabasoglu et al., 2020), ECHAM6.3
 315 (Mauritsen et al., 2019), HADGEM3 (Ridley et al., 2018), MIRCO6 (Kataoka et al., 2020), and CMCC-
 316 CM2 (Cherchi et al., 2019). For each model, we considered the 4 shared socio-economic pathways (SSPs)
 317 that are being used as part of the experiment Coupled Model Intercomparison Project Phase 6, CMIP 6,
 318 of the AR6 (O'Neill et al., 2016). SSP 1 and SSP 5 project a positive development of society, but while
 319 the latter would be at the expense of an economy based on fossil fuel, the former foresees a sustainable
 320 economy. The SSP 2 scenario follows the historical trend, while the SSP 3 and SSP 4 foresee a negative
 321 development of the society dynamics worldwide. Four SSPs scenarios were used in this study, based on
 322 the Representative Concentration Pathways of the AR5, i.e., RCP 2.6, 4.5 and 8.5 scenarios, namely SSP
 323 126, 245, 585 and an intermediate SSP370 scenario. Precipitation was spatially downscaled (i.e. from
 324 GCM cell to rain gauges), with a stochastic space random cascade model (Groppelli et al., 2011a), while
 325 for temperature we used a correction with a mean monthly ΔT approach (Groppelli et al., 2011b).

326 3. Results

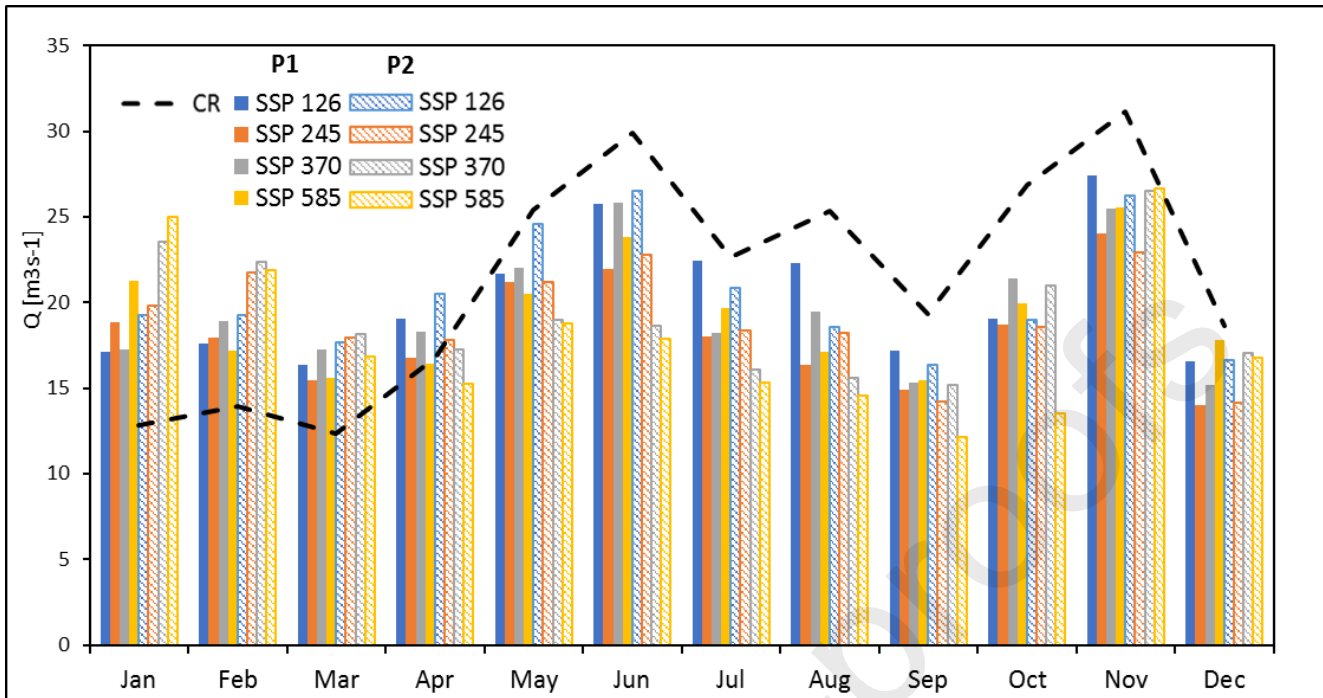
327 3.1. Hydrological modelling and flow projections

328 *Poli-Hydro* model was calibrated to fix the necessary parameters of soil permeability, and snow melting
 329 for a calibration period 2015-2018, by matching Q values as measured at the Ponte Cene hydrometer
 330 (Figure 3). The bias between observed and modelled monthly stream flows was $Bias\% = -7\%$, and NSE
 331 $= 0.71$. Similar statistics values were obtained for the validation period, 2019-2020 ($Bias\% = -6\%$,
 332 $NSE = 0.73$). A table with the calibration parameter of *Poli-Hydro* model is given in the supplementary
 333 material.



334
 335 *Figure 3. Mean monthly flows at Cene Ponte obs/mod during the period 2015-2018.*

336 After model calibration, we used *Poli-Hydro* to assess projected flow discharges. We report in Figure 4
 337 the projected mean monthly flow for each SSP, averaged over the 6 GCMs, at mid-century P1, and end
 338 of century P2, and comparison with discharges in CR period (2012-2021). The increase of liquid
 339 precipitation at the expense of solid precipitation in winter months would lead to an increase of stream
 340 flows therein. The decrease of discharge between May and October would be due to decrease of
 341 precipitation and to a lack of snowmelt and increase of evapotranspiration. Overall, the average annual
 342 discharge ($E[Q_y]$) of $21.26 m^3s^{-1}$ in the CR period, would decrease in the future to $E[Q_y] = 19.19 m^3s^{-1}$,
 343 and $E[Q_y] = 17.83 m^3s^{-1}$ for SSP 585 at P1, and P2, respectively.



344

345

Figure 4. Projected mean monthly flows at Cene Ponte for each SSP at mid-century P1 (solid colour) and end-century P2

346

(striped colour). The black line represents the mean monthly discharge in the CR period.

347

348 3.2. Thermal modelling

349

Poli-Wat.Temp model calibration, namely for parameters α and β , was carried out by minimizing *Bias%*

350

and Random Mean Square Error, *RMSE*. For calibration, starting from the measured water temperature

351

at Fiumenero (1M), we applied the thermal model downstream, and then we corrected the parameters in

352

order to fit the modelled water temperature to observed data in Parre (8V).

353

Then, we calibrated the parameters γ , ω , *Lag*, of Barbellino temperature model by applying *Poli-*

354

Wat.Temp from Barbellino to the first station where we had measured data, i.e. Fiumenero. Here, we

355

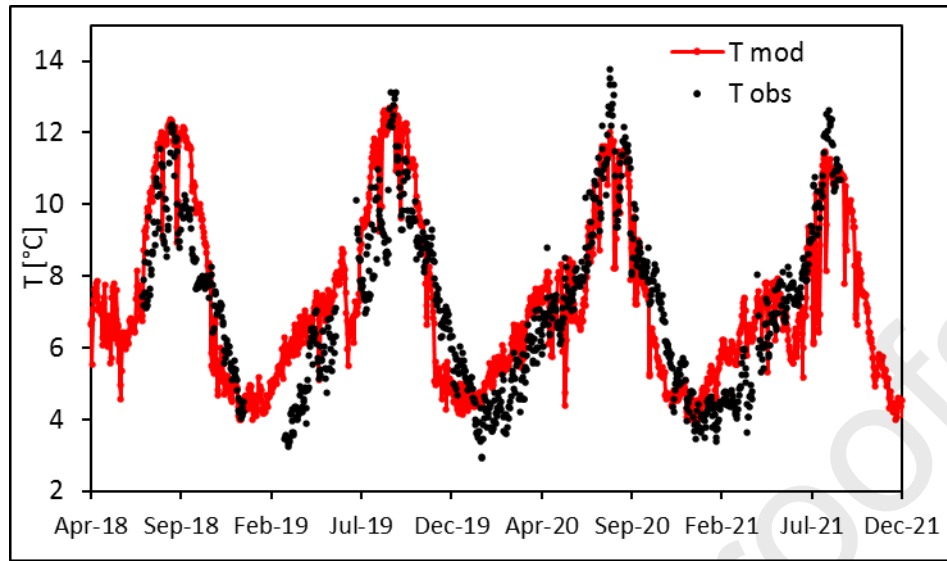
minimized *bias* and *RMSE* of the modelled temperature against the measured data at Fiumenero station

356

(Figure 5). The calibration parameters for the *Poli-Wat.Temp* for Barbellino temperature are shown in

357

the supplementary material (Table 5, Table 6).



358

359

Figure 5 Time serie of estimated water temperature at Fiumenero station (red) vs observed ones (black).

360

Finally, we applied the thermal model from Barbellino to Parre, and we performed model validation, by

361

matching for each station the computed values of water temperature with the measured ones, and

362

evaluating *bias* and *RMSE* thereby (Table 3).

Station	Bias	Std
1M	-0.31	2.06
1V	0.89	2.32
3V	0.07	1.44
3V	0.70	1.74
4	0.33	1.18
6M	-0.15	1.49
6V	-0.06	2.11
8M	-0.16	1.60
8V	-0.12	1.39

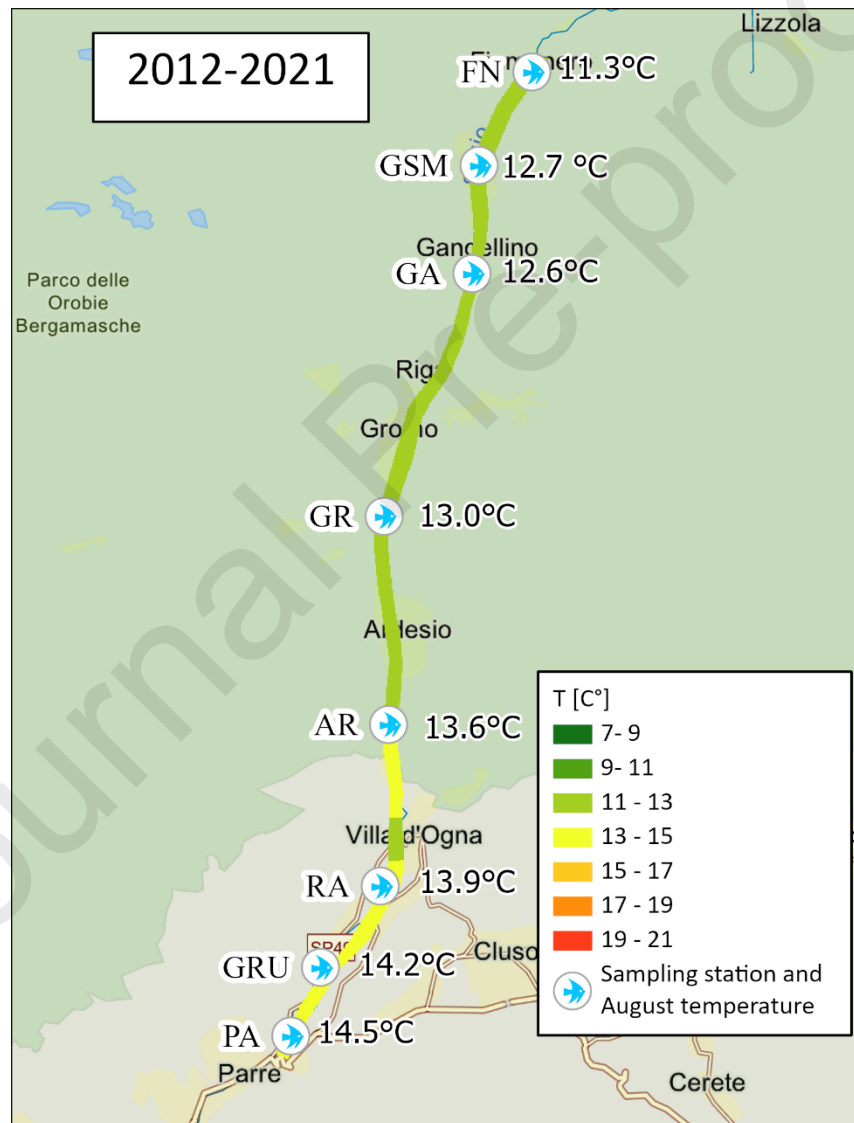
363

Table 3. Values of bias and standard deviation [$^{\circ}\text{C}$] of measured vs modelled temperature at each station of Serio River.

364

365 3.3. Thermal suitability

366 In Figure 6 we report the mean monthly temperature as simulated for the 8 river stations during the CR
 367 period (2012-2021) for the most critical month, i.e. August, when temperatures are the highest (and the
 368 flow the lowest). Although the average temperature is below the critical one for PKD, also in the most
 369 downstream stretch, sporadic exceeding of the threshold is found for the 3 most downstream stations,
 370 where PKD may burst, possibly with low impact.



371

372 *Figure 6. Average water temperature during the CR period (2012-2021) for the whole stretch (color scale) and the*

373

sampling stations (text).

374

375 3.4. Habitat suitability

376 With *Poli-Hydro* model we simulated daily discharges within the 8 sampling locations, and we evaluated
 377 the corresponding PD in each station. In Figure 7 we reported the number of days per year, averaged
 378 along CR period, when trout PD falls in each of the two classes that we defined, i.e. good or poor, based
 379 upon the maximum value of daily potential density PD_{max} . We can see that PD is characterized by higher
 380 variability between the upstream and downstream sections, mainly for adults and juvenile, than for fry.
 381 But for adults, differently from fry and juvenile, most of the downstream sections show seemingly little
 382 suitable habitat conditions, in almost all seasons. Contrarily, for young trout, one finds low habitat
 383 suitability only in the two upstream sections, while overall quite acceptable flow conditions are found.
 384 This is true also for fry, except in downstream sections where habitat is sometimes less suitable.

CR 2012-21

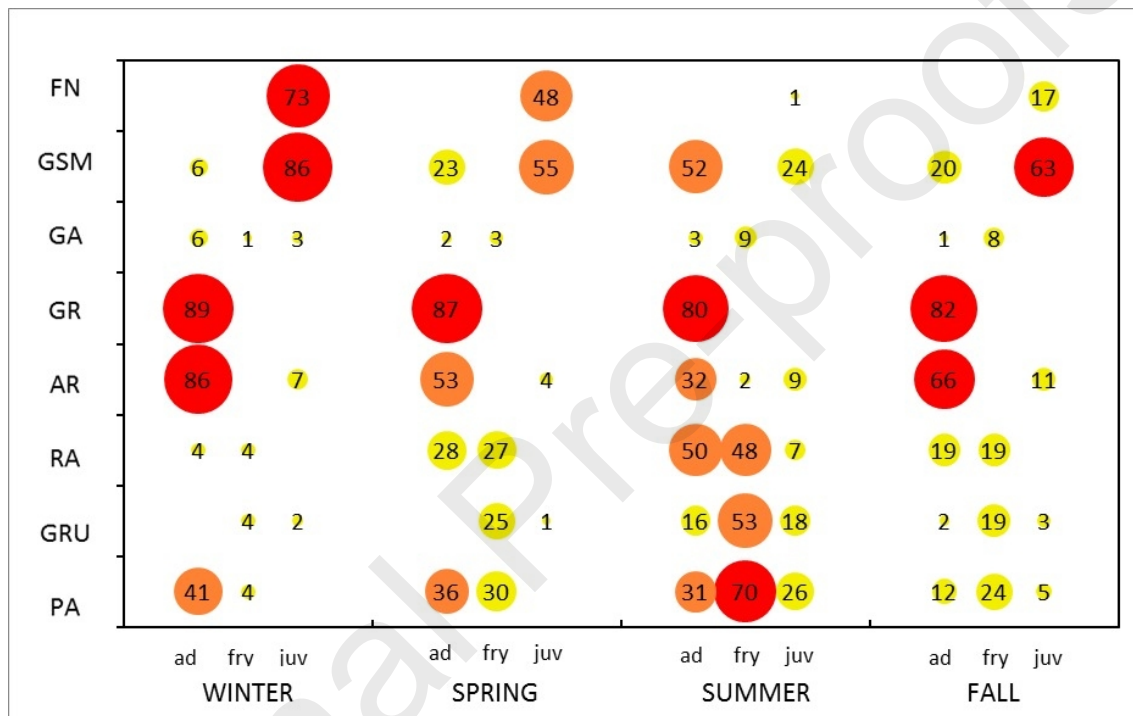
	winter			spring			summer			fall		
	ad	fry	juv	ad	fry	juv	ad	fry	juv	ad	fry	juv
FN	90 0	92 0	18 73	90 0	92 0	44 48	92 0	92 0	91 1	91 0	91 0	74 17
GSM	84 6	92 0	4 86	67 23	92 0	37 55	40 52	92 0	68 24	71 20	91 0	28 63
GA	84 6	91 1	88 3	88 2	89 3	92 0	89 3	92 0	91 1	90 1	83 8	91 1
GR	1 89	92 0	90 0	3 87	92 0	92 0	12 80	92 0	92 0	9 82	91 0	91 0
AR	4 86	92 0	83 7	37 53	92 0	88 4	60 32	92 0	84 8	25 66	91 0	81 10
RA	87 4	89 4	90 0	62 28	65 27	92 0	49 43	92 0	92 0	73 18	73 18	91 0
GRU	90 0	89 4	88 2	90 0	67 25	91 1	92 0	92 0	90 3	91 0	74 18	90 1
PA	49 41	88 4	90 0	54 36	63 30	92 0	82 10	92 0	92 0	84 7	72 19	91 0

386 *Figure 7. Total number of days per year when trout density in each sample station falls within each class, i.e. good (green*
 387 *bar), and poor (red bar), for each season, averaged along the CR period, for each life stage of the trout. Bar width visually*
 388 *indicates the length of the period (over the length of the season, ca. 90 days).*

389

390 3.5. River stress

391 We reported in Figure 8 the river stress indicator, for each sampling site, and trout life stage, averaged
 392 over the CR. Since temperature is nearly always below the PKD critical threshold, the stress conditions
 393 for the river are mainly due to poor habitat suitability. One can see the (negative) contribution of
 394 temperature to RS only in downstream sections and in summer months, where sporadic exceedance of
 395 the thermal threshold is found.



396

397 *Figure 8. River Stress index, expressed in number of days per year, for each season, averaged along the CR period, for*
 398 *each life stage of the trout, at each sampling point. Days 0-30 (yellow), days 30-60 (orange), days 60-90 (red).*

399

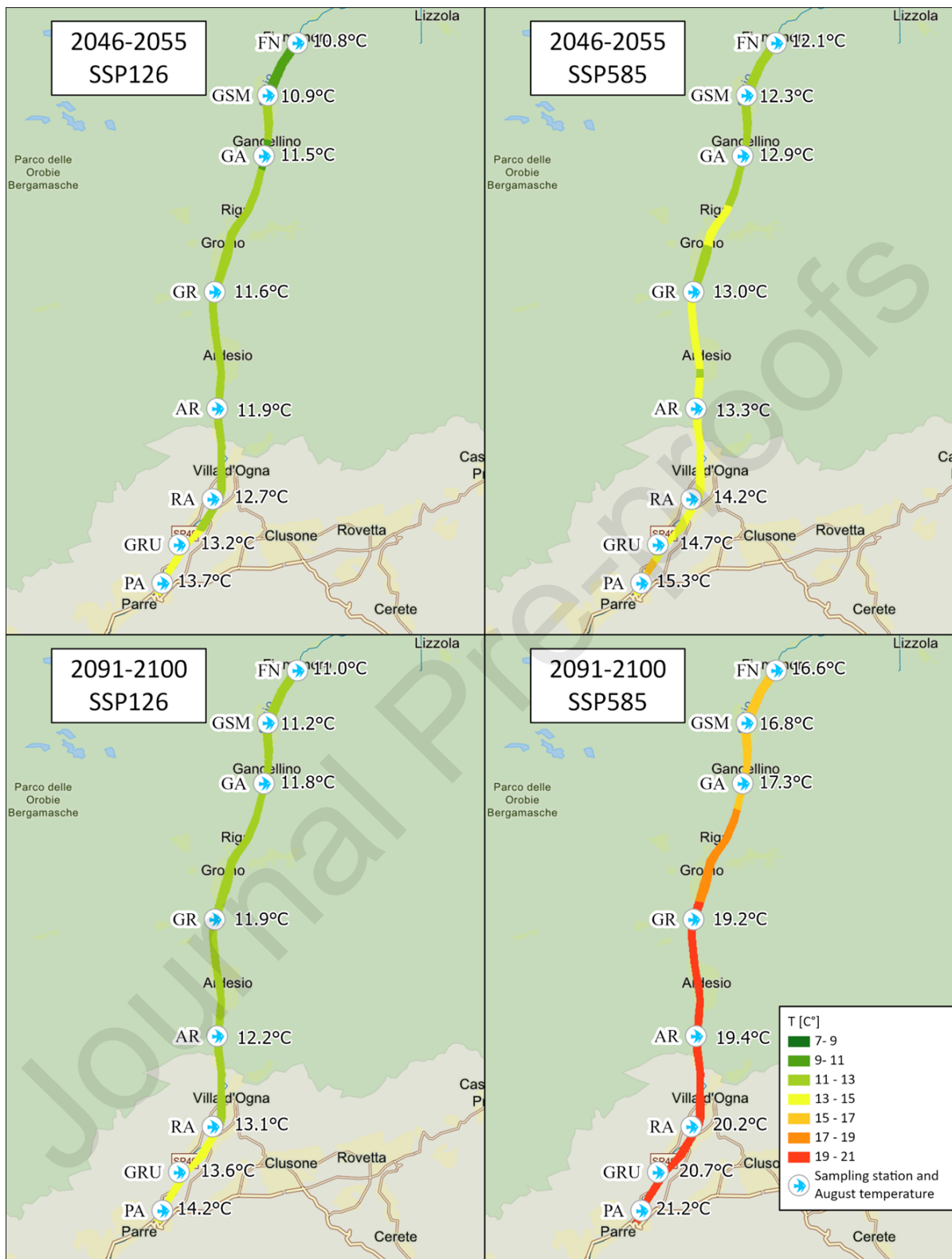
400 3.6. Future thermal suitability

401 Our modelled water temperature in future scenarios is reported for the whole stretch in Figure 9 using
 402 average values of the 6 GCM models only for SSP126, and SSP585, as respectively the more optimistic,
 403 and pessimistic ones, in P1 and P2. One finds that in the worst-case scenario, the model estimated an

404 increase up to +6.5 °C during August, which is again the most critic month, with likely severe
405 consequences on trout health. Indeed, as water temperature would increase, PKD outburst would become
406 more and more frequent, and more severe. In Figure 10 we report the average number of days per year
407 when temperature would be above PKD threshold during CR, under all future scenarios. All scenarios
408 exhibit possible outbreaks. However, while for mid-century P1 spreading of PKD would be limited to
409 most downstream sections, during P2, under the worst scenarios PKD threshold would be exceeded for
410 most of the summer, possibly leading to high mortality in downstream sections, and low mortality
411 elsewhere in the reach.

412

413



414

415 *Figure 9. Average August water temperature for P1 and P2, and 2 scenarios, i.e. SSP 126 in 2046-55, SSP 585 in 2046-55,*

416

SSP 126 in 2091-2100, SSP 585 in 2091-2100.

		CR				2046-55				2091-2100					
		2012-2021	SSP 126	SSP 245	SSP 370	SSP 585	SSP 126	SSP 245	SSP 370	SSP 585	SSP 126	SSP 245	SSP 370	SSP 585	
Possible Outbreak (T > 15 °C for over 14)	FN								54	60					
	GSM								57	66					
	GA								68	73					
	GR							2	82	83					
	AR							5	84	85					
	RA	4				2			22	94	93				
	GRU	6			4	6			35	100	99				
	PA	13		11	12	22			64	104	104				
Low mortality (T > 15 °C for over 29)	FN								53	60					
	GSM								54	63					
	GA								64	73					
	GR								82	83					
	AR							3	84	85					
	RA	4							11	93	93				
	GRU	4			4				23	99	99				
	PA	5		3	5	9			53	103	104				
High mortality (T > 18 °C for over 26)	FN														
	GSM														
	GA								4	7					
	GR								10	13					
	AR								11	14					
	RA								33	41					
	GRU								47	56					
	PA								62	65					

417

418 *Figure 10. Outbreak of PKD in present and future scenarios in 8 considered stations, e.g., average days per year in critical*
419 *conditions. Darker tones of red indicate worse conditions.*

420 To assess hydro-morphological suitability, we evaluated PD for the 8 sampling sites during P1 and P2,
421 for the two scenarios SSP126, and SSP585, thus providing the lower and the upper bound of the future
422 suitability assessment. Then, we evaluated number of days per year, averaged along the CR, P1, and P2,
423 when such weighted PD for the river would fall within each class, for each season (Figure 11). Because
424 winter discharge would increase in future scenarios (Figure 4), water level would also increase, and
425 accordingly adult fish would find more suitable conditions. This projected condition would be confirmed
426 by the slight decrease, in future winters, of the number of days when PD for adult trout would be in
427 “poor” class. On the contrary, in spring and fall, the number of days in “poor” class would remain almost
428 constant, while in summer the critical days would slightly increase. No evident trends are observed for
429 juvenile and fry stages, that may face less criticalities.

P1 SSP 126

	winter			spring			summer			fall		
	ad	fry	juv	ad	fry	juv	ad	fry	juv	ad	fry	juv
FN	71 19	90 0	45 45	49 43	92 0	73 19	28 64	92 0	92 0	71 20	71 20	71 20
GSM	80 10	90 0	15 75	71 21	92 0	52 40	50 43	92 0	92 0	80 11	80 11	80 11
GA	8 82	87 3	89 1	27 65	86 6	89 3	43 49	74 18	74 18	8 83	8 83	8 83
GR	6 84	90 0	90 0	17 75	92 0	92 0	32 60	92 0	92 0	6 85	6 85	6 85
AR	15 75	90 0	81 9	49 43	92 0	81 11	62 31	92 0	92 0	15 76	15 76	15 76
RA	83 7	84 6	90 0	71 21	75 17	92 0	57 35	59 33	59 33	83 8	83 8	83 8
GRU	90 0	85 5	89 1	92 0	77 15	88 4	92 0	62 30	62 30	90 1	90 1	90 1
PA	57 33	84 6	90 0	70 22	73 19	92 0	74 18	57 35	57 35	57 34	57 34	57 34

P1 SSP 585

	winter			spring			summer			fall		
	ad	fry	juv	ad	fry	juv	ad	fry	juv	ad	fry	juv
FN	67 23	90 0	59 31	52 40	92 0	77 16	41 51	92 0	92 0	67 24	67 24	71 20
GSM	74 16	90 0	25 65	74 18	92 0	47 45	66 26	92 0	92 0	74 17	74 17	80 11
GA	15 76	83 7	89 1	21 71	88 4	87 5	28 64	82 10	82 10	15 77	15 77	8 83
GR	12 78	90 0	90 0	11 81	92 0	92 0	19 73	92 0	92 0	12 79	12 79	6 85
AR	25 65	90 0	81 9	43 49	92 0	79 13	46 46	92 0	92 0	25 66	25 66	15 76
RA	76 14	77 13	90 0	79 13	81 11	92 0	71 21	73 19	73 19	76 15	76 15	83 8
GRU	90 0	78 12	87 3	92 0	84 8	87 5	92 0	76 16	76 16	90 1	90 1	90 1
PA	76 14	74 16	90 0	72 20	76 16	92 0	78 14	69 23	69 23	76 15	76 15	57 34

P2 SSP 126

	winter			spring			summer			fall		
	ad	fry	juv	ad	fry	juv	ad	fry	juv	ad	fry	juv
FN	69 21	90 0	51 39	43 49	92 0	77 15	32 60	92 0	92 0	69 22	69 22	69 22
GSM	78 12	90 0	20 71	68 24	92 0	59 33	51 41	92 0	92 0	78 13	78 13	78 13
GA	10 80	84 6	90 0	35 57	85 7	87 5	42 50	78 15	78 15	10 81	10 81	10 81
GR	8 82	90 0	90 0	20 72	92 0	92 0	29 63	92 0	92 0	8 83	8 83	8 83
AR	29 61	90 0	82 8	63 29	92 0	85 7	67 25	92 0	92 0	29 62	29 62	29 62
RA	80 10	81 9	90 0	64 28	68 24	92 0	60 32	64 28	64 28	80 11	80 11	80 11
GRU	90 0	81 9	87 3	92 0	73 19	88 4	92 0	67 25	67 25	90 1	90 1	90 1
PA	56 34	81 9	90 0	71 21	69 23	92 0	79 13	61 31	61 31	56 35	56 35	56 35

P2 SSP 585

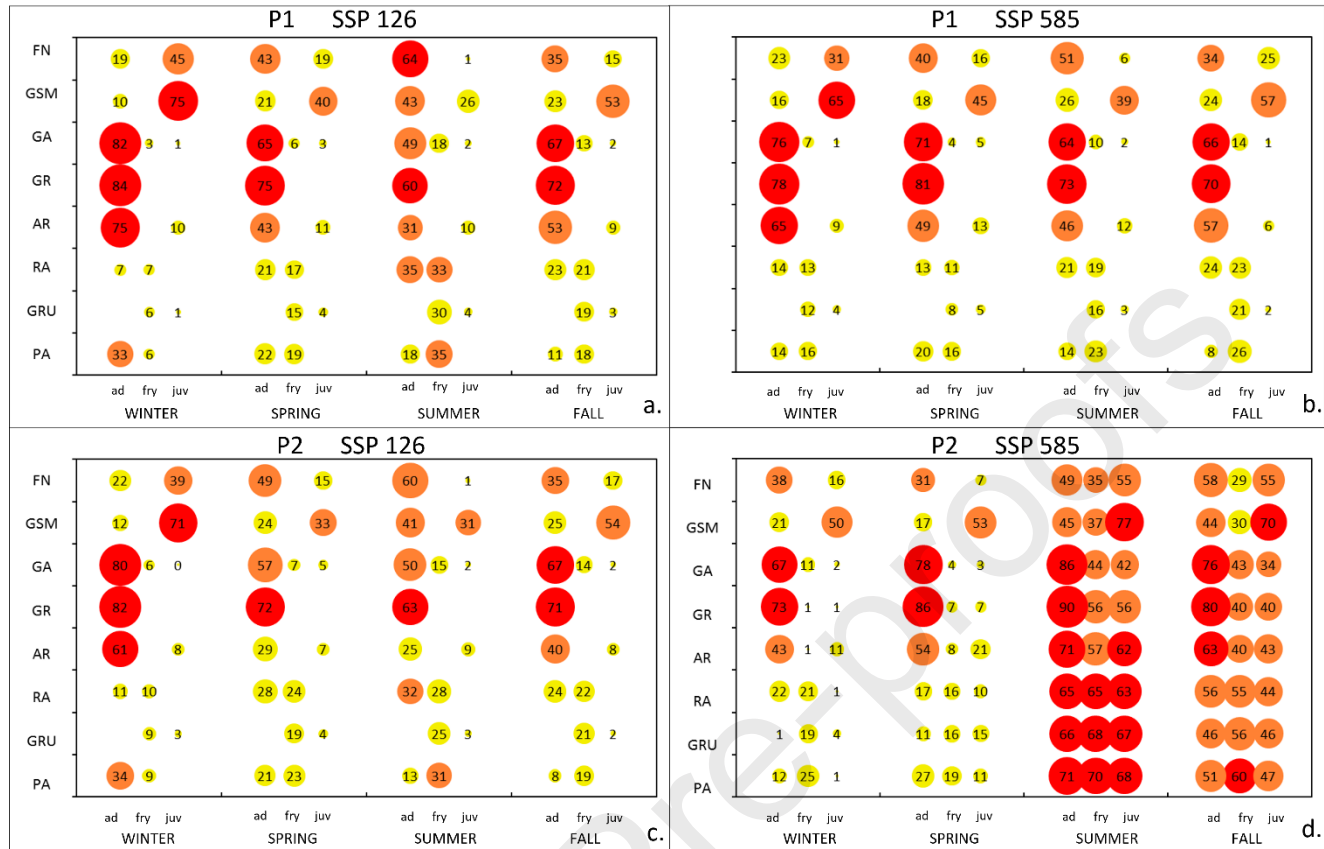
	winter			spring			summer			fall		
	ad	fry	juv	ad	fry	juv	ad	fry	juv	ad	fry	juv
FN	53 38	90 0	74 16	61 31	92 0	85 7	69 23	92 0	92 0	53 39	53 39	53 39
GSM	69 21	90 0	40 50	75 17	92 0	39 53	82 10	92 0	92 0	69 22	69 22	69 22
GA	23 67	79 11	89 2	14 78	88 4	89 3	10 82	89 4	89 4	23 68	23 68	23 68
GR	18 72	90 0	90 0	8 84	92 0	92 0	7 85	92 0	92 0	18 73	18 73	18 73
AR	48 42	90 0	80 10	44 48	92 0	78 15	42 50	92 0	92 0	48 43	48 43	48 43
RA	68 22	69 21	90 0	82 10	83 9	92 0	84 8	85 7	85 7	68 23	68 23	68 23
GRU	90 0	71 19	87 3	92 0	85 7	88 4	92 0	86 6	86 6	90 1	90 1	90 1
PA	79 11	65 25	90 0	75 17	80 12	92 0	85 7	83 9	83 9	79 12	79 12	79 12

431 *Figure 11. Total number of days per year when PD along the river falls within each class, i.e. good (green), and poor (red),*
432 *for each season, averaged on the three decades, CR, half century and end of century, for each life stage of the trout. Bar*
433 *width visually indicates the length of the period (over the length of the season, ca. 90 days).*

434

435 3.7. Future river stress

436 In Figure 12 we report the RS index during P1 and P2, for the two scenarios SSP126, and SSP585.
437 Differently from the findings for the CR period (Figure 8), here the combination of the habitat and
438 thermal suitability seem crucial, since it would lead to a worsening of river conditions when considering
439 both the suitability functions, with respect to the approach of dealing with them separately (Figure 10,
440 Figure 11). Whereas for adult the projected habitat suitability along the river would be undermined under
441 all scenarios both in P1 and P2, for juvenile and fry the findings would be slightly less alarming (Figure
442 11). Contrarily, the RS index, by combining habitat suitability with the effect of projected water
443 temperature increase, would project a picture with larger stress, leading under the worst-case scenarios
444 to the highest stress conditions, in summer and fall seasons.



445

446 *Figure 12. River Stress index, expressed in number of days per year, for each season, for each life stage of the trout, at each*
 447 *sampling point., averaged on P1 and P2, for 2 scenarios, i.e. (a) SSP 126 in 2046-55, (b) SSP 585 in 2046-55, (c) SSP 126*
 448 *in 2091-2100, (d) SSP 585 in 2091-2100. Days 0-30 (yellow), days 30-60 (orange), days 60-90 (red).*

449

450 4. Discussion

451 Suitability indexes depending upon stream flow magnitude, and timing are largely adopted to evaluate
 452 the effect of climate change on riverine habitat (Viganò et al., 2016, Ayllón et al., 2009). However,
 453 assessment of water temperature is likely essential, due to its effects upon physiology and behaviour of
 454 trout (Elliot J. M. and Elliot J. A., 2010). The assessment of water temperature requires proper modelling,
 455 particularly in rivers exploited by human activity, where alteration of the thermal regime as due to
 456 withdrawal, and release is still poorly understood (Dickson et al., 2012). We used here a physically based

457 model, *Poli-Wat.Temp*, depending upon factors directly affecting thermal dynamics. We modelled daily
458 water temperature, obtaining a *Bias* mod/obs smaller than 1°C in each water temperature station, that is
459 consistent with similar studies in nearby areas (Toffolon et Piccolroaz, 2015).

460 In future worst scenarios, we projected a significant temperature increase for water in most downstream
461 areas during August, over +6.5°C, which is even higher than the increase of air temperature as projected.
462 This result is coherent e.g. with a recent study in Columbia basin (Flickin et al., 2014), where the lack of
463 cold water coming from snow would lead to similar temperature outbreaks, and it is also consistent with
464 the historic trend of Swiss streams temperature as observed, nearby +0.37 C° per decade vs +0.13 C° per
465 decade for air temperature (Auer et al., 2007). Nevertheless, in other studies projected temperature
466 increase would be milder (Michel et al., 2022, Agnetti et al., 2018), especially when using empirical
467 models, possibly less recommended for projections in future scenarios (Leach et al., 2019). In these
468 models, generally water temperature is linearly dependant on air temperature with slopes smaller than
469 one (Erickson et al., 1996). However, in physical models the link with air temperature can be more
470 complex, given the presence of other variables also depending upon air temperature, i.e. upstream water
471 temperature like here, and the link between air/water temperatures is less predictable. Here we considered
472 spatial dependence, thus water temperature is affected by upstream boundary conditions, e.g. water
473 temperature in Barbellino lake, with its average linked linearly to annual air temperature. We did not
474 consider here boundary/initial conditions as possibly given by other, smaller reservoirs in the high Serio
475 valley, e.g. Valmorta, Avert. We nevertheless consider this choice as the best option here, since we do
476 not possess data thereby for water temperature assessment. Furthermore, regarding the assessment of
477 Barbellino temperature, the apparent lack of physical modelling of lake heating dynamics, crucial to
478 correctly assess downstream temperature, possibly limits our analysis here. Indeed, most studies
479 concerning lake temperature are related to *epilimnion* (i.e. the lake surface), where more data are

480 available, and remote sensing can be used (Pareeth et al., 2016). Few studies try to model hypolimnion
481 temperature (Prats et al., 2019), and we are not aware of any studies attempting to model lake temperature
482 considering the effect of withdrawal upon lake mixing. Indeed, the morphology of the hydraulic structure
483 impacts lake mixing, and so vertical temperature profile is also affected.

484 According to our predictions of hydro-morphological suitability, we do not foresee very large trends
485 therein for the next future. Like previous studies in the area (Viganò et al., 2016), small flow variations
486 are projected in winter, when a slight increase of discharge, due to larger shares of liquid precipitation,
487 would positively affect adult trout. We observed that potential trout density would never decrease below
488 -40% of its maximum in our simulations, thus dramatic conditions linked to lack of water would not be
489 encountered in Serio River, under our hypotheses. Moreover, the critical periods in response to
490 hydrological and thermal conditions, i.e. winter and summer respectively, do not coincide. Thus, the
491 combined indicator *RS* highlights that the critical periods in the year may be longer than when
492 considering the two suitability indexes separately, as it would be expected. It is important to point out
493 that *RS* we used here was calculated by merging the number of days when *PD* falls in “poor” class, and
494 the number of days when water temperature is above the threshold for the possible outbreak of PKD. If
495 we had considered the intersection of the two sets, or a different criterion to define the critical threshold
496 for temperature, probably the results would be less critical. However, we considered the lowest
497 temperature threshold for PKD because it is the one likely to be most sensitive to climate change. Three
498 years of water temperature monitoring (2018-2021) in the Upper Serio catchment revealed an acceptable
499 thermal habitat for *Salmo trutta*, since water temperature was always below the chosen critical thresholds.
500 The future projections show continuous, and evident worsening of the thermal habitat for trout, in
501 particular for most downstream stations (RA, GRU, PA).

502 Other studies recently demonstrated the worsening of thermal conditions in temperate rivers due to
503 climate change. Santiago et al. (Santiago et al., 2016) studied the effects of climate change upon the
504 thermal niche of brown trout in the Iberian Duero River basin. They showed that in the worst scenario
505 (RCP 8.5), loss of habitat of brown trout may reach -30% in the upstream part of the basin, at the end of
506 the century. The thermal niche was assessed using a threshold based on the exceeding of +18°C (daily
507 mean), and projections showed an increase of ca. 3 and 9 folds of the number of consecutive days above
508 the threshold, with RCP 4.5, and 8.5 respectively. Similarly, Borgwardt et al. (2020) projected the effects
509 of climate change on Austrian brown trout at country scale, assessing both physiological stress, and
510 potential emergence of diseases. Overall, they found that at the end of the century, RCP 8.5 would show
511 an increase of both high mortality (+25%) and low mortality (+20%) conditions. In our case study, high
512 mortality ($T_w > 18^\circ\text{C}$) is seldom, if ever, predicted since we studied a cold Alpine river. However, our
513 results clearly show that the habitat of brown trout would face a more dramatic condition, with headwater
514 areas becoming the only optimal niche for the conservation of the species.

515 We consider the PKD as the most likely risk factor for trout, preliminarily neglecting a possible negative
516 effect as due to lack of food, or hypoxia. Indeed, several studies demonstrated that increasing
517 temperatures enhance disease prevalence, severity and distribution, and PKD-related mortality (Okamura
518 201; Waldner et al., 2019). By contrast, rising temperatures do not seem to adversely affect food
519 availability, because secondary productivity of benthos generally increases (Albertson et. al., 2018;
520 Bonacina, 2022). Furthermore, as aforementioned, oxygen rate in the Serio River was always found at
521 saturation level, likely due to flow turbulence, and the maximum temperatures projected in the worst
522 scenario (approximately +21°C) did not visibly cause a decrease in oxygen below the concentration
523 needed by trout (7 mg/l). Sub-Alpine and Alpine rivers are profoundly impacted by human
524 infrastructures, both for hydroelectric and irrigation purposes, affecting the riverine thermal regime

525 (Cassie, 2006). For this reason, we included here hydropower diversion in our study. To further explore
526 climate change impacts upon fish communities, more detailed investigation covering the effects of plants
527 and dams on the thermal regime should be carried out at a regional scale.

528 This study helps to understand the magnitude of thermal impacts and explores measures to mitigate the
529 effects of global warming. For instance, an increase of the minimum flow discharge, especially during
530 summer heat waves, could increase the thermal inertia of the river and reduce warming, decreasing the
531 number of critical days, possibly at the cost of reducing hydropower production. Moreover, other
532 strategies to reduce temperature raising could be implemented, such as the increase of vegetation cover
533 along the river to enhance the shading and reduce the effect of solar radiation.

534 Here we considered as a target species the *Salmo trutta*, since it is regarded as a most abundant, and
535 economically viable fish species in Serio River. However, the marble trout (*Salmo marmoratus*),
536 indigenous and subendemic of the Po Valley (Zerunian, 2003), has the same habitat preferences of the
537 allopatric brown trout, and it may survive to higher temperature thresholds, so in the future it might likely
538 face less criticalities. Marble trout is included in the Habitat Directive (92/43/CEE), and in the IUCN
539 Red List of Threatened species (Crivelli, 2006). Another endemic species of the Po Valley is *Cottus*
540 *gobio* (Elliot J. et Elliot A., 1995) also included in the Habitat Directive (92/43/CEE), as well in the
541 IUCN Red list of vertebrate animals (Rondinini et al., 2013), and it has more flexible thermal preference
542 compared to *Salmo trutta*. Thus, the conservation of the endangered species *Salmo marmoratus* and
543 *Cottus gobio* may be fundamental to maintain healthy fish communities on subalpine rivers like Serio
544 here, also under a climate change adaptation perspective.

545

546 **5. Conclusions**

547 This study introduces a new physical model to assess river water temperature with the presence of
548 hydropower plants, and a synthetic *River Stress* index to consider both the effects of change in discharge
549 and water temperature on riverine habitat. The proposed methodology was applied to alpine Serio River
550 in present and IPCC future scenarios, where future hydraulic habitat suitability is not expected to
551 highlight large criticalities, while projections of stream temperature show apparently more alarming
552 findings.

553 This methodology can be applied to other Alpine rivers, also exploited for human activities and requiring
554 quality assessment, pending basic information availability of hydrology, thermal regime, and fish
555 abundance, as reported here. Even in lack of information, some findings may be portable to other areas,
556 e.g. fish density functions for similar target species. Such analysis may help in i) evaluating seasonal
557 criticalities for fish species, and ii) providing more sustainable withdrawal strategies and, thus outlining
558 a background for planning adaptation strategies.

559

560 **Author Contributions:** Conceptualization, F.F. and L.S.; data collection: L.B, R.F; models set up and
561 calibration, F.F., L.S., L.B.; writing—original draft preparation, F.F., and L.S.; supervision, D.B., and
562 R.F.; review and editing, D.B. All authors have read and agreed to the published version of the
563 manuscript.

564 **Funding:** This research did not receive any specific grant from funding agencies in the public,
565 commercial, or not-for-profit sectors.

566 **Acknowledgements:** Flavia Fuso acknowledges support from *Gruppo CAP Holding* Milano for her
567 PhD, through the scholarship *Assessment of hydrological flows in Lombardy Alpine rivers, and their*
568 *connection with the underground aquifer, under potential climate change scenarios in the XXI century.*
569 Leonardo Stucchi acknowledges support from ERSAF Lombardia-Direzione Parco dello Stelvio, within

570 the project “*Progetto IDROSTELVIO - Un network per il monitoraggio e la modellazione del ciclo*
571 *idrologico nel Parco dello Stelvio Lombardo*”, and from GE.RI.KO. Mera Interreg Project, Interreg Italia
572 Svizzera 2014/2020. Personnel of *Climate-Lab*, the interdisciplinary laboratory on climate change of
573 Politecnico di Milano (www.climatelab.polimi.it/) is kindly acknowledged for the support with hardware
574 for calculation, and for *in situ* activity.

575 The authors thank Valeria Mezzanotte, Francesca Marazzi, Marco Mantovani, helping with sampling
576 activity, field measurements, and useful suggestions. Three anonymous reviewers are kindly
577 acknowledged for helping to improve the manuscript.

578 **Conflicts of Interest:** The authors declare no conflict of interest.

579

581 **References**

- 582
583 Agnetti, A., Tugnoli, F., Pecora, S, 2018. Prediction of the thermal regime of the Po river under climate
584 change. Proc of the 5th IAHR Europe Congress-New challenges in hydraulic research and engineering.
585 Trento. doi:10.3850/978-981-11-2731-1_349-cd
- 586 Albertson, L.K., Ouellet, V., Daniels, M. D. 2018. Impacts of stream riparian buffer land use on water
587 temperature and food availability for fish. *Journal of Freshwater Ecology*. 195-210 DOI:
588 10.1080/02705060.2017.1422558
- 589 Armour, C., L., 1994. Evaluating Temperature Regimes for Protection of Brown Trout. U.S. department
590 of the interior national biological survey. Resource Publication 201.
- 591 Arnell, N. W., 1999. The effect of climate change on hydrological regimes in Europe: a continental
592 perspective. *Global Environmental Change*, 9, 5-23. [http://dx.doi.org/10.1016/S0959-3780\(98\)00015-6](http://dx.doi.org/10.1016/S0959-3780(98)00015-6)
- 593 Auer, I., Böhm, R., Jurkovic, A., Lipa, W., Orlik, A., Potzmann, R., Schöner, W., Ungersböck, M.,
594 Matulla, C., Briffa, K., Jones, P., Efthymiadis, D., Brunetti, M., Nanni, T., Maugeri, M., Mercalli, L.,
595 Mestre, O., Moisselin, J.-M., Begert, M., Müller-Westermeier, G., Kveton, V., Bochnicek, O., Stastny,
596 P., Lapin, M., Szalai, S., Szentimrey, T., Cegnar, T., Dolinar, M., Gajic-Capka, M., Zaninovic, K.,
597 Majstorovic, Z. and Nieplova, E., 2007. HISTALP—historical instrumental climatological surface time
598 series of the Greater Alpine Region. *Int. J. Climatol.*, 27, 17-46. <https://doi.org/10.1002/joc.1377>
- 599 Ayllón, D., Almodóvar, A., Nicola, G., G., Elvira, B., 2009. Interactive effects of cover and hydraulics
600 on brown trout habitat selection patterns *River Res. Appl.*, 25, 1051-
601 1065. <https://doi.org/10.1002/rra.1215>
- 602 Benyahya, L., Caissie, D., St-Hilaire, A., Ouarda, T., Bobee, B., 2007. A review of statistical water
603 temperature Models. *Canadian water resources Journal*, 32, 179-192.
604 <https://doi.org/10.4296/cwrj3203179>

- 605 Bocchiola, D., 2014. Long term (1921-2011) changes of Alpine catchments regime in Northern Italy.
606 *Advances in Water Resources*, 70, 51-64. <https://doi.org/10.1016/j.advwatres.2014.04.017>
- 607 Bocchiola, D., Diolaiuti, G., 2010. Evidence of climatic trends in the Adamello glacier of Italy. *Theor.*
608 *App. Clim.*, 100, 351-69. 10.1007/s00704-009-0186-x
- 609 Borgwardt F., Unfer, G., Auer, S., Waldner, K., El-Matbouli M., Bechter T., 2020. Direct and Indirect
610 Climate Change Impacts on Brown Trout in Central Europe: How Thermal Regimes Reinforce
611 Physiological Stress and Support the Emergence of Diseases. *Frontiers in Environmental Science*, 8.
612 <https://doi.org/10.3389/fenvs.2020.00059> <https://doi.org/10.3389/fenvs.2020.00059>
- 613 Borsuk, M. E., Reichert, P., Peter, A., Schager, E., & Burkhardt-Holm, P. (2006). Assessing the decline
614 of brown trout (*Salmo trutta*) in Swiss rivers using a Bayesian probability network. *Ecological*
615 *Modelling*, 192(1-2), 224-244.
- 616 Bustillo, V., Moatar, F., Ducharne, A., Thiery, D., Poirel, A., 2015. A multimodel comparison for
617 assessing water temperatures under changing climate conditions via the equilibrium temperature concept:
618 case study of the Middle Loire River, France. *Hydrological Processes*, 28, 1507-1524. 10.1002/hyp.9683
- 619 Caissie, D., El-Jabi, N., Satish, M., 2001. Modelling of maximum daily water temperatures in a small
620 stream using air temperatures. *Journal of hydrology*, 251, 14-28. 10.1016/S0022-1694(01)00427-9
- 621 Caissie, D., El-Jabi, N., Satish, M., 2005. Predicting water temperatures using the equilibrium
622 temperature concept with Application on Miramichi River catchments. *Hydrological Process*, 19, 2137-
623 2159.
624 <https://doi.org/10.1002/hyp.5684>
- 625 Caissie, D., El-Jabi, N., St-Hilaire, A., 1998. Stochastic modelling of water temperatures in a small
626 stream using air to water relations. *Canadian Journal of Civil Engineering*, 25, 250-260.
627 <https://doi.org/10.1139/197-091>

- 628 Caissie, D., 2006 The thermal regime of rivers: a review. *Freshwater Biology*, 51, 1389-1406 doi:j.1365-
629 2427.2006.01597x
- 630 Canobbio, S., Azzellino, A., Cabrini, R., and Mezzanotte, V., 2013. A multivariate approach to assess
631 habitat integrity in urban streams using benthic macroinvertebrate metrics. *Water Sci. Technol.*, 67,
632 2832–2837. <https://doi.org/10.2166/wst.2013.166>
- 633 Carraro, L., Bertuzzo, E., Mari, L., Fontes, I., Rinaldo, A., 2017. Integrated field, laboratory, and
634 theoretical study of PKD spread in a Swiss prealpine river. *PNAS*, 114, 11992-
635 11997. <https://doi.org/10.1073/pnas.1713691114>
- 636 Cherchi, A., Fogli, P. G., Lovato, T., Peano, D., Iovino, D., Gualdi, S., 2019. Global mean climate and
637 main patterns of variability in the CMCC-CM2 coupled model. *Journal of Advances in Modeling Earth*
638 *Systems*, 11, 185– 209. <https://doi.org/10.1029/2018MS001369>
- 639 Crivelli, A.J., 2006. *Salmo marmoratus*. The IUCN Red List of Threatened Species.
640 <http://dx.doi.org/10.2305/IUCN.UK.2006.RLTS.T19859A9043279.en>.
- 641 Danabasoglu, G., Lamarque, J.F., Bacmeister, J., Bailey, D.A., DuVivier, A.K., Edwards, J., Emmons,
642 L.K., Fasullo, J., Garcia, R., Gettelman, A., Hannay, C., Holland, M.M., Large, W.G., Lauritzen, P.H.,
643 Lawrence, D.M., Lenaerts, J.T.M., Lindsay, K., Lipscomb, W.H., Mills, M.J., Neale, R., Oleson, K.W.,
644 Otto-Bliesner, B., Phillips, A.S., Sacks, W., Tilmes, S., van Kampenhout, L., Vertenstein, M., Bertini,
645 A., Dennis, J., Deser, C., Fischer, C., Fox-Kemper, B., Kay, J.E., Kinnison, D., Kushner, P.J., Larson,
646 V.E., Long, M.C., Mickelson, S., Moore, J.K., Nienhouse, E., Polvani, L., Rasch, P.J., Strand, W.G.,
647 2020. The Community Earth System Model Version 2 (CESM2). *J. Adv. Model. Earth Syst.*
648 <https://doi.org/10.1029/2019MS001916>
- 649 Deas, M., L., Lowney, C., L., 2000. *Water Temperature Modeling Review, Central Valley.*

- 650 Dickson, N., E., Carrivick, J., L., Brown, L., E., 2012. Flow regulation alters alpine river thermal regimes.
651 *Journal of Hydrology*, 464, 505-516. <https://doi.org/10.1016/j.jhydrol.2012.07.044>
- 652 Dodds, W., Whiles, M., 2010. *Freshwater Ecology: concepts and environmental applications of*
653 *Limnology*. 2nd Edition.
- 654 Doll, P., Zhang, J., 2010. Impact of climate change on freshwater ecosystems: a global scale analysis of
655 ecologically relevant river flow alterations. *Hydrology and Earth System Sciences*, 14, 783-799.
656 <https://doi.org/10.5194/hess-14-783-2010>
- 657 EC-Earth Consortium (EC-Earth), 2019. EC-Earth-Consortium EC-Earth3-Veg model output prepared
658 for CMIP6 ScenarioMIP'. Version 22/10/2020. Earth Syst. Grid Fed.
659 <https://doi.org/https://doi.org/10.22033/ESGF/CMIP6.727>
- 660 Edinger, J., Duttweile, D., W., Geyer, J., C., 1968. The Response of Water Temperatures to
661 Meteorological Conditions. *Water Resources Research*, 4, 1137-1143.
- 662 Elliot, J., Elliot, A., 1995. The critical thermal limits for the bullhead, *Cottus Gobio*, from three
663 populations in north-west England. *Freshwater biology*, 33, 411-418. [https://doi.org/10.1111/j.1365-](https://doi.org/10.1111/j.1365-2427.1995.tb00403.x)
664 [2427.1995.tb00403.x](https://doi.org/10.1111/j.1365-2427.1995.tb00403.x)
- 665 Elliott, J., M., Elliot, J., A., 2010. Temperature requirements of Atlantic salmon *Salmo salar*, brown trout
666 *Salmo trutta* and Arctic charr *Salvelinus alpinus*: predicting the effects of climate change. *Journal of Fish*
667 *Biology*, 77, 1793-1817. <https://doi.org/10.1111/j.1095-8649.2010.02762.x>
- 668 Erickson, T., R., Stefan, H., G., 1996. Correlations of Oklahoma Stream Temperatures with Air
669 Temperatures. St. Anthony Falls Laboratory. Retrieved from the University of Minnesota Digital
670 Conservancy, <https://hdl.handle.net/11299/109509>.
- 671 EU Biodiversity Strategy for 2030, European Commission, Brussels 2020.

- 672 Ficklin, D. L., Barnhart, B. L., Knouft, J. H., Stewart, I. T., Maurer, E. P., Letsinger, S. L., and Whittaker,
673 G. W., 2014. Climate change and stream temperature projections in the Columbia River basin: habitat
674 implications of spatial variation in hydrologic drivers, *Hydrol. Earth Syst. Sci.*, 18, 4897–4912.
675 <https://doi.org/10.5194/hess-18-4897-2014>
- 676 Fishery Planning of Bergamo Province. 2009.
677 [https://www.regione.lombardia.it/wps/wcm/connect/696a9055-ba7b-4e71-9f78-
678 56c4012dc691/Piano+ittico+2009.pdf?MOD=AJPERES&CACHEID=ROOTWORKSPACE-
679 696a9055-ba7b-4e71-9f78-56c4012dc691-IHSFuNX](https://www.regione.lombardia.it/wps/wcm/connect/696a9055-ba7b-4e71-9f78-56c4012dc691/Piano+ittico+2009.pdf?MOD=AJPERES&CACHEID=ROOTWORKSPACE-696a9055-ba7b-4e71-9f78-56c4012dc691-IHSFuNX)
- 680 Fornaroli, R., Cabrini, R., Sartori, L., Marazzi, F., Canobbio, S., Mezzanotte, V., 2016. Optimal Flow
681 for Brown Trout: Habitat-Prey Optimization. *Science of the Total Environment*, 566, 1568–78.
682 <http://dx.doi.org/10.1016/j.scitotenv.2016.06.047>.
- 683 Fornaroli, R., Cabrini, R., Sartori, L., Marazzi, F., Vraceutic, D., Mezzanotte, V., Annala, M., Canobbio,
684 S., 2015. Predicting the constraint effect of environmental characteristics on macroinvertebrate density
685 and diversity using quantile regression mixed model. *Hydrobiologia*, 742, 153–167.
686 <https://doi.org/10.1007/s10750-014-1974-6>
- 687 Fuso, F., Casale, F., Giudici, F., Bocchiola, D., 2020. Future hydrology of the cryospheric driven Lake
688 Como catchment in Italy under climate change scenarios. *Climate*, 9, 8.
689 <https://doi.org/10.3390/cli9010008>
- 690 Gropelli, B., Bocchiola, D., Rosso, R., 2011a. Spatial downscaling of precipitation from GCMs for
691 climate change projections using random cascades: A case study in Italy. *Water Resour. Res.*
692 <https://doi.org/10.1029/2010WR009437>

- 693 Groppelli, B., Confortola, G., Soncini, A., Bocchiola D., Rosso, R., 2011. Assessment of future river
694 habitat suitability under climate change scenarios in a mesoscale Alpine watershed of Italy (Serio River,
695 Italian Alps). American Geophysical Union. Fall meeting.
- 696 Groppelli, B., Soncini, A., Bocchiola, D., Rosso, R., 2011b. Evaluation of future hydrological cycle under
697 climate change scenarios in a mesoscale Alpine watershed of Italy. *Nat. Hazards Earth Syst. Sci.*
698 <https://doi.org/10.5194/nhess-11-1769-2011>
- 699 Hondzo, M., Stefan, H., G., 1993. Regional water temperature characteristics of lakes subjected to
700 climate change. *Climatic Change*, 24, 187-211. <https://doi.org/10.1007/BF01091829>
- 701 Isaak, D., J., Luce, C., H., Rieman, B., E., Nagel, D., E., Peterson, E., E., Horan, D., L., Parkes, S.,
702 Chandler, G.,L., 2010. Effects of climate change and wildfire on stream temperatures and salmonid
703 thermal habitat in a mountain river network. *Ecological Applications*, 20, 1350-1371.
704 <https://doi.org/10.1890/09-0822.1>
- 705 Jonsson, B., Jonsson, N., 2009. A review of the likely effects of climate change on anadromous Atlantic
706 salmon *Salmo salar* and brown trout *Salmo trutta*, with particular reference to water temperature and
707 flow. *Journal of fish biology*, 75, 2381-2447. <https://doi.org/10.1111/j.1095-8649.2009.02380.x>
- 708 Kataoka, T., Tatebe, H., Koyama, H., Mochizuki, T., Ogochi, K., Naoe, H., Imada, Y., Shiogama, H.,
709 Kimoto, M., Watanabe, M., 2020. Seasonal to Decadal Predictions with MIROC6: Description and Basic
710 Evaluation. *Journal of Advances in Modeling Earth Systems*, 12.
711 <https://doi.org/10.1029/2019MS002035>.
- 712 Kedra, M., Wiejaczka, L., 2017. Climatic and dam-induced impacts on river water temperature:
713 Assessment and management implications. *Science of the total environment*, 6262, 1474-1483.
714 <https://doi.org/10.1016/j.scitotenv.2017.10.044>

- 715 Lamouroux, N., Capra, H., Pouilly, M., 1998. Predicting habitat suitability for lotic fish: Linking
716 statistical hydraulic models with multivariate habitat use models. *Regulated rivers: research and*
717 *management*, 4, 1-11. [https://doi.org/10.1002/\(SICI\)1099-1646\(199801/02\)14:1<1::AID-RRR472>3.0.CO;2-D](https://doi.org/10.1002/(SICI)1099-1646(199801/02)14:1<1::AID-RRR472>3.0.CO;2-D)
- 719 Lamouroux, N., Cattaneo, F., 2006. Fish assemblages and stream hydraulics: Consistent relations across
720 spatial scales and regions. *River research and applications*, 22, 727-737. <https://doi.org/10.1002/rra.931>
- 721 Leach, J., A., Moore, R., D., 2019. Empirical stream thermal sensitivities may underestimate stream
722 temperature response to climate warming. *Water Resources Research*, 55, 5453– 5467.
723 <https://doi.org/10.1029/2018WR024236>.
- 724 Lehner, B., Doll, P., Alcamo, J., Henrichs, T., Kaspar, F., 2006. Estimating the Impact of Global Change
725 on Flood and Drought Risks in Europe: A Continental, Integrated Analysis. *Climatic Change*, 75, 273-
726 299. <https://doi.org/10.1007/s10584-006-6338-4>
- 727 Mauritsen, T., Bader, J., Becker, T., Behrens, J., Bittner, M., Brokopf, R., Brovkin, V., Claussen, M.,
728 Crueger, T., Esch, M., Fast, I., Fiedler, S., Fläschner, D., Gayler, V., Giorgetta, M., Goll, D.S., Haak, H.,
729 Hagemann, S., Hedemann, C., Hohenegger, C., Ilyina, T., Jahns, T., Jimenéz-de-la-Cuesta, D., Jungclaus,
730 J., Kleinen, T., Kloster, S., Kracher, D., Kinne, S., Kleberg, D., Lasslop, G., Kornblueh, L., Marotzke,
731 J., Matei, D., Meraner, K., Mikolajewicz, U., Modali, K., Möbis, B., Müller, W.A., Nabel, J.E.M.S.,
732 Nam, C.C.W., Notz, D., Nyawira, S.S., Paulsen, H., Peters, K., Pincus, R., Pohlmann, H., Pongratz, J.,
733 Popp, M., Raddatz, T.J., Rast, S., Redler, R., Reick, C.H., Rohrschneider, T., Schemann, V., Schmidt,
734 H., Schnur, R., Schulzweida, U., Six, K.D., Stein, L., Stemmler, I., Stevens, B., von Storch, J.S., Tian,
735 F., Voigt, A., Vrese, P., Wieners, K.H., Wilkenskjaeld, S., Winkler, A., Roeckner, E., 2019. Developments
736 in the MPI-M Earth System Model version 1.2 (MPI-ESM1.2) and Its Response to Increasing CO₂. *J.*
737 *Adv. Model. Earth Syst.* 11, 998–1038. <https://doi.org/10.1029/2018MS001400>

- 738 Meier, W., Bonjour, C., Wüest, A., Reichert, P., 2003. Modelling the Effect of Water Diversion on the
739 Temperature of Mountain Streams. *Journal of Environmental Engineering*, 129, 8.
740 doi:10.1061/(ASCE)0733-9372(2003)129:8(755)
- 741 Michel, A., Schaepli, B., Wever, N., Zekollari, H., Lehning, M., and Huwald, H., 2022. Future water
742 temperature of rivers in Switzerland under climate change investigated with physics-based models,
743 *Hydrol. Earth Syst. Sci.*, 26, 1063–1087. <https://doi.org/10.5194/hess-26-1063-2022>
- 744 Morid, R., Shimatani, Y., Sato, T, 2020. An integrated framework for prediction of climate change
745 impact on habitat suitability of a river in terms of water temperature, hydrological and hydraulic
746 parameters. *Journal of hydrology*, 587. <https://doi.org/10.1016/j.jhydrol.2020.124936>
- 747 Nukazawa, K., Schiraiwa, J.I., Kazama, S., 2011. Evaluations of seasonal habitat variations of freshwater
748 fishes, fireflies, and frogs using a habitat suitability index model that includes river water temperature.
749 *Ecological modelling*, 222, 3718-3726. <https://doi.org/10.1016/j.ecolmodel.2011.09.005>
- 750 Nurnberg, G., 2007. Lake responses to long-term hypolimnetic withdrawal treatments. *Lake and*
751 *Reservoir Management*, 23, 388-409. <https://doi.org/10.1080/07438140709354026>
- 752 O'Neill, B.C.; Tebaldi, C., Van Vuuren, D.P., Eyring, V., Friedlingstein, P., Hurtt, G., Knutti, R.,
753 Kriegler, E., Lamarque, J.F. Lowe, J., et al. 2016. The Scenario Model Intercomparison Project
754 (ScenarioMIP) for CMIP6. *Geosci. Model Dev.* 9, 3461–3482, doi:10.5194/gmd-9-3461
- 755 Pareeth, S., Salmaso, N., Adrian, R., 2016. Homogenised daily lake surface water temperature data
756 generated from multiple satellite sensors: A long-term case study of a large sub-Alpine lake. *Sci*
757 *Rep* 6, 31251. <https://doi.org/10.1038/srep31251>
- 758 Parra, I., Almodovar, A., Ayllon, D., Nicola, G.G., Elvira, B., 2012. Unravelling the effects of water
759 temperature and density dependence on the spatial variation of brown trout (*Salmo trutta*) body size.
760 *Canadian journal of fisheries and aquatic sciences*, 69, 821-832. <https://doi.org/10.1139/f2012-025>

- 761 Pellicciotti, F., Brock, B., Strasser, U., Burlando, P., Funk, M., Corripio, J., 2005. An enhanced
762 temperature-index glacier melt model including the shortwave radiation balance: development and
763 testing for Haut Glacier d'Arolla, Switzerland. *J. Glaciol.* 51, 573–587.
764 <https://doi.org/10.3189/172756505781829124>.
- 765 Prats, J., Danis, P.A., 2019 An epilimnion and hypolimnion temperature model based on air temperature
766 and lake characteristics. *Knowledge & Management of Aquatic Ecosystems.* 420, 8.
767 <https://doi.org/10.1051/kmae/2019001>
- 768 Lombardy Region. Regolamento regionale 22/9/2003.
- 769 Ridley, J., Menary, M., Kuhlbrodt, T., Andrews, M., 2018. Andrews, Tim. MOHC HadGEM3-GC31-
770 LL model output prepared for CMIP6 CMIP. Earth System Grid Federation.
771 <https://doi.org/10.22033/ESGF/CMIP6.419>
- 772 Rondinini, C., Battistoni, A., Peronace, V., Teofili, C., 2013. Lista Rossa IUCN dei Vertebrati Italiani.
773 Comitato Italiano IUCN e Ministero dell'Ambiente e della Tutela del Territorio e del Mare, Roma.
- 774 Saber, A., James, D., E., Hayes, D., F., 2019. Long-term forecast of water temperature and dissolved
775 oxygen profiles in deep lakes using artificial neural networks conjugated with wavelet transform.
776 *Limnology and oceanography*, 65, 1297-1317. <https://doi.org/10.1002/lno.11390>
- 777 Santiago, J., M., Jalon, D., G., Alonso, C., Solana, J., Ribalaygua, J., Pórtoles, J., Monjo, R., 2016.
778 Brown trout thermal niche and climate change: expected changes in the distribution of cold-water fish in
779 central Spain. *Ecohydrology*, 9, 514-528. <https://doi.org/10.1002/eco.1653>
- 780 Soncini, A., Bocchiola, D., Azzoni, R.S., Diolaiuti, G., 2017. A methodology for monitoring and
781 modeling of high altitude Alpine catchments. *Prog. Phys. Geogr.* 41, 393–420.
782 <https://doi.org/10.1177/0309133317710832>

- 783 Sperna Weiland, F., C., Van Beek, L., P., Kwadijk, J., C., Bierkens, M., F., 2012. Global patterns of
784 change in discharge regimes for 2100. *Hydrology and Earth System Sciences*, 16, 1047-1062.
785 <https://doi.org/10.5194/hess-16-1047-2012>
- 786 Toffolon M., Piccolroaz, S., 2015. A hybrid model for river water temperature as a function of air.
787 *Environmental Research Letters*, 10 . <https://doi.org/10.1088/1748-9326/10/11/114011>
- 788 Van Vliet, M., T., H., Franssen, W., H., P., Yearsley, J., R., Ludwig, F., Haddeland, I., Lettenmaier, D.,
789 P., Kabat, P., 2013. Global river discharge and water temperature under climate change. *Global*
790 *Environmental Change*, 23, 450-464. <https://doi.org/10.1016/j.gloenvcha.2012.11.002>
- 791 VanCompernelle, M., Knouft, J., Ficklin, D., 2019. Hydrologic and thermal conditions occupied by a
792 species within a single watershed predict the geographic extent of occurrence of freshwater fishes.
793 *Ecohydrology*, 12. <https://doi.org/10.1002/eco.2071>
- 794 Viganò, G., Confortola, G., Fornaroli, R., Cabrini, R., Canobbio, S., Mezzanotte, V., Bocchiola, D., 2016.
795 Effects of Future Climate Change on a River Habitat in an Italian Alpine Catchment. *Journal of*
796 *hydrologic engineering*, 21, 2. doi/full/10.1061/%28ASCE%29HE.1943-5584.0001293
- 797 Vorosmarty, C., j., Green, P., Salisbury, J., Lammers, R., B., 2000. Global Water Resources:
798 Vulnerability from Climate Change and Population Growth. *Sciences*, 289, 284-288. DOI:
799 10.1126/science.289.5477.284
- 800 Waldner, K, Bechter, T, Auer, S, Borgwardt, F, El-Matbouli, M, Unfer, G. A brown trout (*Salmo trutta*)
801 population faces devastating consequences due to proliferative kidney disease and temperature increase:
802 A case study from Austria. *Ecol Freshw Fish*. 2020; 29: 465– 476. <https://doi.org/10.1111/eff.12528>
- 803 Wahli, T., Bernet, D., Steiner, P.A. *et al.* Geographic distribution
804 of *Tetracapsuloides bryosalmonae* infected fish in Swiss rivers: an update. *Aquat. Sci.* **69**, 3–10 (2007).
805 <https://doi.org/10.1007/s00027-006-0843-4>

806 Webb, B., W., Hannah, D., M., Dan Moore, R., Brown, L., E., Nobilis, F., 2008. Recent advances in
807 stream and river temperature research. *Hydrological Processes*, 22, 902-
808 918. <https://doi.org/10.1002/hyp.6994>

809 Zerunian S., 2003. Piano d'azione generale per la conservazione dei Pesci d'acqua dolce italiani. *Quad.*
810 *Cons. Natura*, 17, Min. Ambiente - Ist. Naz. Fauna Selvatica.

811 Zhu S., Nyarko E., K., Hadzima-Nyarko M., 2018. Modelling daily water temperature from air
812 temperature for the Missouri River. *PeerJ*, 6. <https://doi.org/10.7717/peerj.4894>

813

Journal Pre-proofs

814

815 Supplementary material

Parameter	Unit	Description	Value	Method
DDS	$[\text{mmd}^{-1} \text{ } ^\circ\text{C}^{-1}]$	Degree Day Snow	5	Literature [42]
t_g, t_s	[h]	Lag times, ground/surface	50, 400	Calibration, Hydrograph shape
n_g, n_s	[-]	Reservoirs, ground/surface	3, 3	Literature [41]
K	$[\text{mmd}^{-1}]$	Saturated conductivity	3	Calibration, flow volumes
k	[-]	Ground flow exponent	0.5	Calibration, flow volumes
θ_w, θ_s	[-]	Water content, wilting, field capacity	0.15, 0.45	Literature [41]

816

Table 1. Parameters for Poli-Hydro calibration.

817

Parameter	Unit	Value
α	$[\text{JK}^{-1}\text{m}^{-3}]$	20.94
β	[s]	41.87

818

Table 2. Calibration parameter of the thermal model, Eq. (2)

819

Parameter	Unit	Value
γ	[-]	0.35
ω	[-]	0.5
Lag	[day]	105

820

Table 3. Calibration parameter of the Barbellino lake temperature model, Eq. (6)

821

- 822 • Climate change is leading to hydro-thermal river regimes unsustainable to salmonids.
- 823 • We couple a new physically based thermal model, *Poli-Wat.Temp* with hydrological model *Poli-*
824 *Hydro*, to assess water temperature as a function of air temperature, and river discharge.
- 825 • We constrain habitat suitability against water temperature, by assessing a synthetic River Stress
826 index
- 827 • With respect to a solely habitat based assessment, the Rivers Stress index highlights longer critical
828 periods per year.
- 829 • The increase in water temperature will result into worse conditions for trouts in summer.

830

831